Chapter 2. Present understanding of compressional wave properties

Compressional wave properties of marine sediments have been measured by a large number of authors, using a variety of techniques (see *Chapter 3* for detailed discussion). These measurements have been used to enhance our understanding of the propagation of compressional waves through marine sediments, by examining their frequency-dependence, validating physical models and identifying empirical relationships with geotechnical properties.

In order to properly investigate compressional waves in marine sediments measurements made must span a range of sediment types and frequencies. One manner of achieving such a range, which is adopted by a number of authors, is to gather together compilations of data. Such compilations incorporate a range of research projects, which use different techniques to examine different sediment types and frequencies. Hence any examination of the dependence of a compressional wave property on either frequency or a single physical property suffers from the presence of latent variables, which introduce a degree of variability. It is questionable if the direct comparison of data obtained from a range of sources is a valid approach. The approach used in this project will avoid such compilations.

2.1. Definitions

Compressional waves (otherwise known as longitudinal waves) are waves in which the particles are displaced parallel to the direction of motion of the wave. As in all cases of wave propagation, it is the wave that travels away from the source, while the particles simply oscillate about a fixed point. The compressional wave properties of interest to this project are the compressional wave velocity, attenuation coefficient and quality factor. Though these properties are discussed with respect to compressional waves, the following definitions are equally applicable to other forms of wave propagation, *e.g.* shear and surface waves.

Velocity: For an infinitely long sinusoidal wave propagating in a single direction the phase velocity v_{ph} is defined as

$$v_{ph} = f\lambda = \frac{\omega}{\kappa} \qquad 2.1,$$

where f is the frequency, λ the wavelength, ω the angular frequency and κ the wave number.

Though an infinitely long wave is an excellent theoretical concept, acoustic experiments use more practical pulses of waves. These can be considered to be constructed from a superposition of a set of infinite waves which possess different frequencies and amplitudes. In a dispersive media, *i.e.* one in which phase velocity is frequency-dependent, higher frequency components will typically possess higher phase velocities. Hence as the pulse propagates through the medium the pulse will spread out, *Figure 2.1.* The velocity of the pulse is measured by the group velocity v_g, which is determined from

$$v_g = \frac{\partial \omega_o}{\partial \kappa_o} \qquad 2.2,$$

where ω_o is the dominant angular frequency and κ_o the dominant wave number. In the remainder of this thesis velocity will be denoted by v, with the type of velocity specified in the text. As a general rule of thumb the velocities predicted by theoretical models will be phase velocities, while those measured by experiments will typically be group velocities.

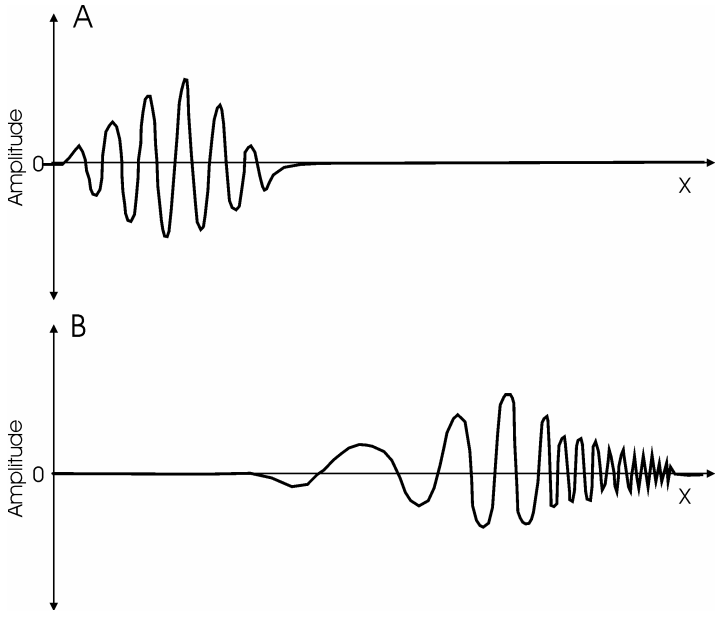

Figure 2.1. Schematic of the propagation of an acoustic pulse through a dispersive medium, displaying the initial pulse shape (A) and the pulse at some transmission distance later (B). Note the reshaping and spreading of pulse due to higher frequencies travelling at a higher phase velocity. From (Leighton, 1994).

Attenuation coefficient and loss mechanisms: Consider a wave which has been emitted by a source and is propagating through a medium. After a distance x and time *t* the amplitude of the wave *A(x,t)* will be

$$A(x,t) = A_O \cdot G(x) \cdot e^{-\alpha_n x} \cdot e^{i(kx-\omega t)} \qquad 2.3,$$

where A_o is the amplitude at $t=0$ and $x=0$, α_n is the attenuation coefficient in nepers·m^{-1} and *G(x)* accounts for the spreading losses of the source used. The first exponential term represents the attenuation of the medium, while the second represents the wave oscillations. The attenuation coefficient in nepers·m^{-1} can therefore be obtained from

$$\alpha_n = \frac{1}{x_2 - x_1} \ln\left(\frac{A(x_1) \cdot G(x_2)}{A(x_2) \cdot G(x_1)}\right) \qquad 2.4,$$

where $A(x_1)$ and $A(x_2)$ are the amplitudes of waves that have propagated through distances x_1 and x_2 respectively, and $G(x_1)$ and $G(x_2)$ are the corresponding spreading corrections.

Alternatively attenuation coefficient can be expressed in dB·m^{-1} using

$$\alpha = \frac{1}{x_2 - x_1} 20 \cdot \log_{10}\left(\frac{A(x_1) \cdot G(x_2)}{A(x_2) \cdot G(x_1)}\right) = 8.686 \cdot \alpha_n \qquad 2.5,$$

where α denotes the attenuation coefficient in dB·m^{-1}.

Several sources of energy loss mechanisms exist in marine sediments, with the attenuation coefficient measured dependent on the experiment performed. These include energy loss due to conversion of acoustic energy into heat energy (*i.e.* frictional and viscous losses) and additional mechanisms. Frictional losses occur at grain-to-grain boundaries due to relative motion of mineral grains, and produce attenuation coefficients which are proportional to frequency and increase as the strain amplitude applied increases (Cascante, 1996). Viscous forces arising from the relative motion of the pore fluid and solid frame also result in the dissipation of energy. Such losses occur on both global and local scales, with global flow favoured in high permeability sediments at low frequencies and local, or squirt, flow favoured in less permeable sediments at higher frequencies (see *Section 2.5.2* for more detailed discussion). Additional mechanisms include: volume scattering losses from both individual grains and larger scale heterogeneities, interfaces losses from reflectors and refractors, and the conversion of energy to shear and interface waves.

The mechanisms incorporated by the attenuation coefficient will depend on the experiment performed. In well-sorted sediment examined under laboratory conditions the

attenuation coefficient measured will include frictional and viscous losses only and is termed the *intrinsic* attenuation coefficient. Field experiments on *in situ* sediments are more likely to measure an *effective* attenuation coefficient (Stoll, 1985), as they include scattering and interfaces losses as well as frictional and viscous losses. Finally, the original version of Biot Theory considered within this thesis (see *Section 2.5.2* for details*)* will predict absorption coefficients, which incorporate viscous losses only.

Quality factor: Quality factor Q is an additional measure of energy loss and is defined as the inverse fractional energy loss per cycle, *i.e.*

$$Q = \frac{2\pi \cdot E}{\Delta E} \qquad 2.6,$$

where E is the mean energy per cycle and ΔE is the energy loss per cycle. As the energy of a wave is proportional to the amplitude squared *Equations 2.3* and *2.6* can be combined to produce

$$Q = \frac{2\pi}{1 - e^{-2\alpha_n \lambda}} \qquad 2.7.$$

The exponential term can be expanded in a power series and in the case of "small damping" only the first term need be retained (Johnstone and Toksoz, 1981), resulting in the following approximation for Q

$$Q = \frac{\pi f}{\alpha_n v} \qquad 2.8.$$

This approximation is valid for quality factors much greater than unity (Johnstone and Toksoz, 1981), which for the purposes of this thesis are deemed to be quality factors greater than 10.

The **geotechnical properties** of interest are divided into the more basic properties which are measured within this project (*Appendix C*), *i.e.* grain size parameters, porosity and bulk density, and the more technical properties which are obtained from either empirical relationships or valid ranges in literature (*Section 7.1.3*), *i.e.* bulk and shear moduli, fluid viscosity and permeability. Only those properties which are measured will be defined in this section, with the more technical properties discussed later in the relevant model sections.

All natural sediments possess a range of grain sizes and so a grain size distribution. Standard statistical techniques are used to examine these distributions, with the common features obtained being the mean grain diameter, M, and the sorting, σ, of the distribution.

In addition, the percentage of sand sized particles is often used, where sands are defined as particles with a grain diameter between 63 μm and 2 mm (McManus, 1989).

The percentage porosity n of saturated sediment is defined by

$$n = 100 \cdot \frac{V_W}{V_T} \qquad 2.9,$$

where V_W is the volume of pore water and V_T the total volume of the sediment. Hence the porosity represents the fraction of a saturated sediment which consists of pore water. Due to the highly compressible nature of the pore water with respect to that of the sediment frame, the porosity has a fundamental effect on compressional wave properties (Hamilton, 1970).

The bulk density ρ of the sediment can be calculated from

$$\rho = \frac{n}{100}\rho_f + \left(1 - \frac{n}{100}\right)\rho_r \qquad 2.10,$$

where ρ_f is the density of the pore water and ρ_r the density of the mineral grains.

2.2. Typical sediment structures

The structure of the sediment will affect both the geotechnical and compressional wave properties and varies with sediment type. Sands form structures in which the relative positions of particles are controlled by gravitational forces and the dominant force between the particles is friction at grain-to-grain contacts, *Figure 2.2A*. Packing controls porosity, with porosities varying from 26 to 47.6 % for equal sized spheres and 37 to 57 % for more angular sands containing a range of grain sizes (Hamilton, 1987).

The introduction of small amounts of finer materials, such as clays and silts, results in the finer material settling in the pore spaces between larger sand particles, *Figure 2.2B*, which will decrease porosity. Alternatively the introduction of platy minerals, such as biotite, can result in a bridging effect, *Figure 2.2C,* and an increase in porosity. As the percentage of fine-grained material increases a critical porosity will be reached where the sand particles become suspended in a silt/clay matrix and the fine-grained particles dominate the sediment structure.

Fine silts and clays contain adsorbed water and hence interparticle Van-der-Waals forces dominate over frictional forces. Upon deposition on the seafloor these particles will adhere to the first particles they come in contact with and resulting forces will maintain

this arrangement and produce a three-dimensional structure, *Figure 2.2D* to *2.2F*. The combination of adhered water and a more open structure results in higher porosities than in sands. The most frequently observed structure in continental shelf sediments is the packet structure, *i.e.* particles stacked face-to-face to form packets which are linked by relatively short chains of particles.

An additional factor controlling the structure of fine-grained sediments is the clay mineralogy. Clay minerals that dominate marine sediments are montmorillonite, illite and kaolinite. As the surface area to mass ratio of montmorillonite is at least an order of magnitude greater than that of illite or kaolinite, sediment containing montmorillonite has a much higher porosity than those containing other clay minerals, with computations indicating an increase of between 5 and 13 % (Hamilton, 1970).

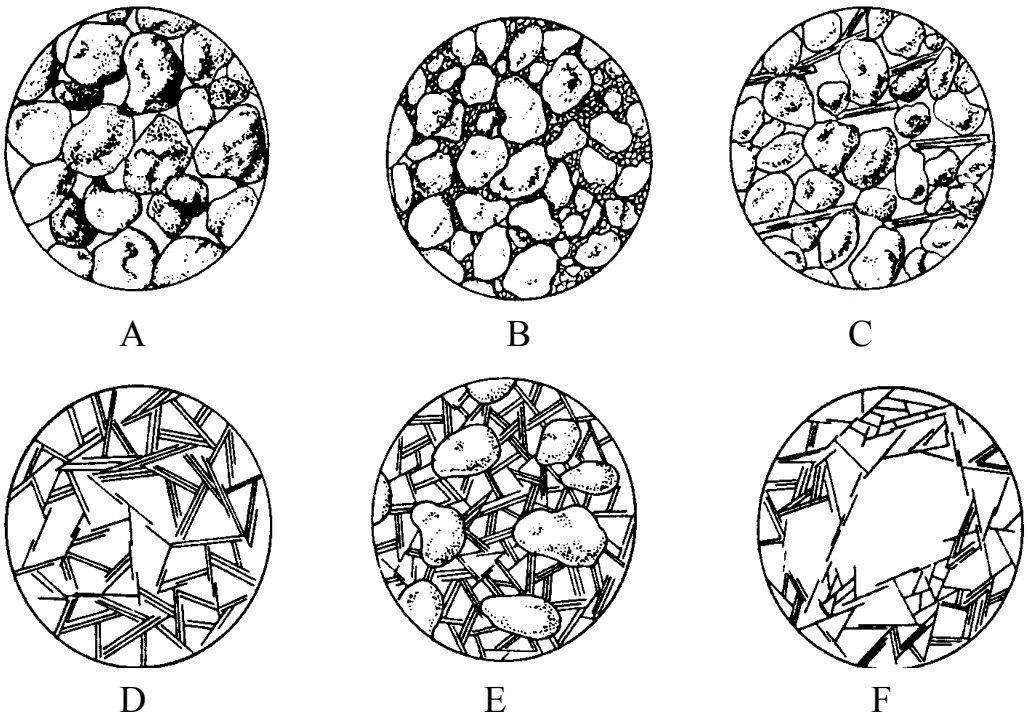

Figure 2.2. Typical sediment structures including; a well-sorted sand (A), a mixture of sand and clay (B and E), the possible bridging effect of biotite particles (C) and fine grained sediments (D and F). From (Hamilton, 1987).

These structural variations within sediments result in an increase in porosity as mean grain diameter decreases, *Figure 2.3*, a relationship which has been experimentally

confirmed by a number of authors (Bachman, 1985; Courtney and Mayer, 1993b; Hamilton, 1970; Hamilton, 1971b; Orsi and Dunn, 1990). The increased porosity of diatomaceous sediments, which results from the bridging effects of platy biotite minerals, can also be observed within *Figure 2.3.*

As defined in *Equation 2.10,* bulk density depends on the density of the sediment grains, density of pore water and their relative proportions. Continental shelf sediments consist of a small number of common minerals, which are predominantly from terrigenous sources. These include quartz, feldspars, calcite, micas, clay minerals and very minor amounts of certain heavy minerals (Hamilton, 1987). As the grain densities of these common minerals vary from 2000 to 2800 $kg \cdot m^{-3}$, and marine sediments predominantly consist of either quartz or calcite, the density of most mineral aggregates found in marine sediments is limited to 2650 and 2750 $kg \cdot m^{-3}$ (Hamilton and Bachman, 1982). The density of pore water displays negligible changes over the range of temperatures, pressures and salinities observed in marine sediments with values ranging from 1000 to 1030 $kg \cdot m^{-3}$ (Courtney and Mayer, 1993a; Stoll, 1985). Hence the dominant parameter affecting bulk density is porosity.

A number of authors, (Bachman, 1985; Hamilton, 1970; Orsi and Dunn, 1991; Richardson and Briggs, 1993) have examined the interrelationship between density and both porosity and mean grain diameter. As *Equation 2.10* predicts, bulk density increases in a linear manner as porosity decreases, *Figure 2.4.* The negligible scatter of the data points from the expected linear relationship highlights that porosity is the dominant factor controlling bulk density. Bulk density increases as mean grain diameter increases, *Figure 2.5,* though the increased scatter of data implies that this a secondary effect. The scatter arises from the range of grain size distributions, which can possess the same mean grain diameter and porosity. Though alternative measures of grain diameter, *e.g.* the percentage of sand sized particles, may provide better indices with which porosity and density can be compared, there is at present insufficient evidence in the published literature to confirm this hypothesis.

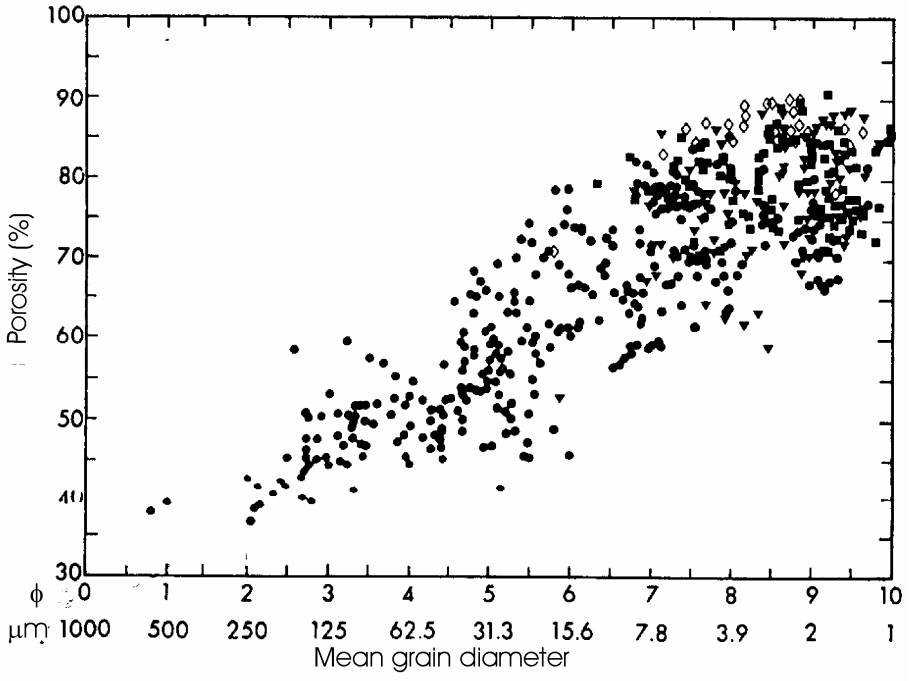

Figure 2.3. Relationship between porosity and mean grain size for range of samples for the three general sediment environments of continental shelf (circles), abyssal hills (squares) and abyssal plain (triangles). Diatomaceous sediments are displayed as open diamonds and mean grain diameter is expressed in units of ϕ and μm. From (Hamilton, 1987).

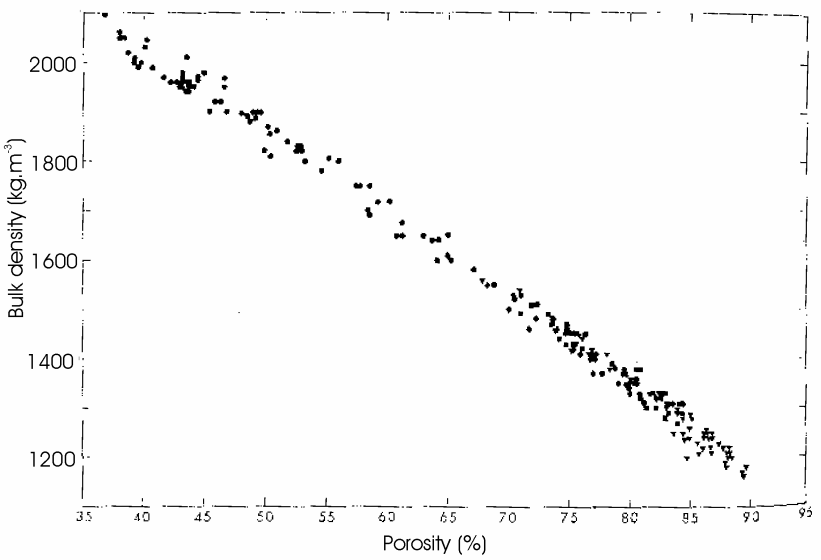

Figure 2.4. Relationship between bulk density and porosity for three sediment environments: continental shelf (circles), abyssal hills (squares) and abyssal plain (triangles). From (Hamilton, 1975).

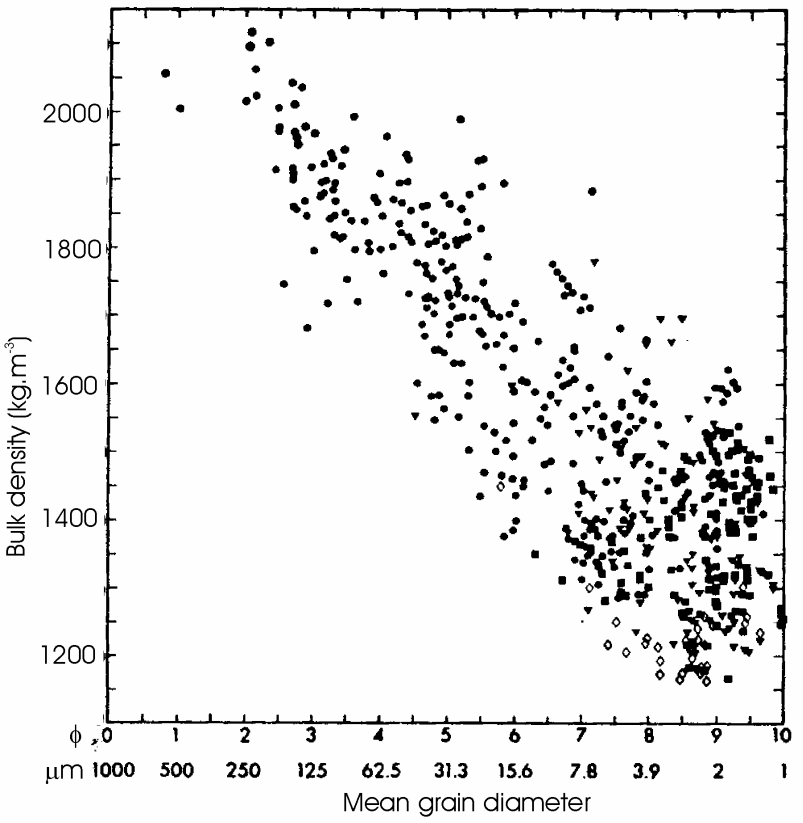

Figure 2.5. Relationship between bulk density and mean grain diameter for three sediment environments: continental shelf (circles), abyssal hills (squares) and abyssal plain (triangles). Diatomaceous sediments are displayed as open diamonds. From (Hamilton, 1987).

2.3. Variation of compressional wave properties with frequency

2.3.1. Frequency-dependence of velocity

Previous research projects which measure compressional wave velocity over a range of frequencies are summarised in *Table 2.1.* Though a suite of work observes negligible dispersion in artificial or reconstituted sediments (Hamilton, 1972; McLeroy and DeLoach, 1968), the omission of error analysis from the relevant literature casts doubt on the conclusions drawn. *In situ* measurements also observe negligible velocity dispersion (Best *et al.*, 2001; Hamilton, 1972), though the errors associated are able to conceal dispersions of 0.3 and 7 % respectively, while laboratory experiments at frequencies of 375 to 935 kHz observe no dispersion within errors from ± 2 to ± 20 $m \cdot s^{-1}$ (McCann, 1967).

Frequency (kHz)	Velocity range	Degree of dispersion	Sediment type	Reference
0.2 – 73	N/a	N	sand (artificial)	(Hamilton, 1972)
15 – 1500	$1.189 \cdot v_w$	N	silt-clay to sand (reconstituted)	(McLeroy and DeLoach, 1968)
0.2 – 4.7	1410 – 1740 $m \cdot s^{-1}$	N	*Silt* (in situ)	(Best *et al.*, 2001)
14 - 100	1704 – 1712 $m \cdot s^{-1}$	N	Sand *(in situ)*	(Hamilton, 1972)
375 - 935	1560 – 1741 $m \cdot s^{-1}$	N	Sand to clay *(*laboratory)	(McCann, 1967)
50 – 350	N/a	0.5 %	Sand (reconstituted)	(Wingham, 1985)
3 – 200	$0.93 \cdot v_w$ – $0.99 \cdot v_w$	4 – 6 %	Silt/clay (artificial)	(Hampton, 1967)
25 – 100	1727 – 1797 $m \cdot s^{-1}$	4 %	Sand *(in situ)*	(Buckingham and Richardson, 2002)
20 – 100	N/a	25 $m \cdot s^{-1}$	Sand *(in situ)*	(Gorgas *et al.*, 2002)
1 - 30	1580 – 1720 $m \cdot s^{-1}$	8.9 %	Sand *(in situ)*	(Turgut and Yamamoto, 1990).
0.125 – 50	1580 – 1755 $m \cdot s^{-1}$	11.1 %	Sand *(in situ)*	(Stoll, 2001)
0.125 - 400	$1.05 \cdot v_w$ – $1.17 \cdot v_w$	11.4 %	Sand *(in situ)*	(Williams *et al.*, 2002)

Table 2.1. Summary of compressional wave velocity measurements which span a range of frequencies. N denotes no dispersion.

An alternative suite of literature supports varying degrees of dispersion. The relevance of the dispersion observed for artificial or reconstituted sediments (Hampton,

1967; Wingham, 1985) to *in situ* sediments is debatable due to the unknown disturbance of the samples examined. More reliable *in situ* measurements obtained from a single device and survey show dispersions less than 8.9 % in sands (Buckingham and Richardson, 2002; Gorgas *et al.*, 2002; Turgut and Yamamoto, 1990), with a larger degree of dispersion occurring for the lower frequency range of 1 to 30 kHz. Finally two compilations of velocities, which arise from a similar suite of devices and techniques, observe dispersions from 11.1 to 11.4 %. The close agreement in the levels of dispersion observed and large discrepancy in the frequencies examined by these compilations imply that velocity dispersion is more pronounced at lower frequencies than at higher frequencies. However, the observation of varying degrees of dispersion from different devices and surveys within these compilations casts doubt on the compilation approach adopted, while the omission of published error analysis in certain cases (Stoll, 2001; Turgut and Yamamoto, 1990; Williams *et al.*, 2002) prevents overall conclusions concerning dispersion from being drawn.

Values of dispersion obtained through the comparison of velocities measured at low frequencies using *in situ* techniques and at higher frequencies using laboratory techniques (Best *et al.*, 2001; Gorgas *et al.*, 2002; Richardson *et al.*, 1997) are omitted owing to the differences in the measurement techniques used and degrees of disturbance induced.

2.3.2. Frequency-dependence of attenuation coefficient and quality factor

The frequency-dependence of attenuation coefficient is typically examined using

$$\alpha = k_A f^q \qquad 2.11,$$

where k_A is the constant of proportionality and q is the exponent of frequency (Hamilton, 1972). Measurements of compressional wave attenuation coefficients in marine sediments over a range of frequencies are summarised in *Table 2.2.* These vary from 2.2×10^{-4} dB·m^{-1} at frequencies of 50 Hz to 200 dB·m^{-1} at frequencies of 400 kHz. Pre-1980 research generally reports an attenuation coefficient which is proportional to frequency (Bennett, 1967; Hamilton, 1972; Lewis, 1971; McCann and McCann, 1969; McLeroy and DeLoach, 1968; Wood and Weston, 1964). This research is combined with additional measurements at discrete frequencies to extend this linear relationship to the MHz range (Hamilton, 1972). However, several issues are raised concerning this research, which include:

- The adoption of a compilation approach which incorporates attenuation coefficients obtained from a range of devices, techniques and sediment types.
- Exponents of frequency derived from certain individual sources that either deviate from unity (Hamilton, 1972; McCann and McCann, 1969; Wood and Weston, 1964) or lack statistical validation (Bennett, 1967; McLeroy and DeLoach, 1968; Neprochnov, 1971).
- The frequency range spanned by individual surveys is typically less than one decade. If the scatter in attenuation coefficient is considered, it is impossible to accurately determine frequency dependence (Stoll, 1985). This is highlighted by a compilation of attenuation coefficients from fine-grained sediment (Bowles, 1997) which presents an optimum exponent of 1.12, *Figure 2.6*. However, within 95 % confidence limits, it is impossible to distinguish between an exponent of unity, the optimum exponent of 1.12 or the variable frequency-dependence predicted by Biot-Stoll Theory (see *Section 2.5.2* for a detailed discussion).
- Attenuation coefficients measured at low frequencies of 5 Hz to 250 Hz have been added to Hamilton's compilation of attenuation coefficients (Kibblewhite, 1989; Stoll, 1985). These are lower than those predicted by the linear interpolation, *Figure 2.7,* and so cast doubt on attenuation coefficients that are directly proportional to frequency.

Attenuation coefficients which do not vary with frequency in a linear manner are observed by a number of authors (Best *et al.*, 2001; Courtney and Mayer, 1993a; Evans and Carey, 1998; Shumway, 1960). Doubt is raised in the highly variable exponents of 0.6 to 3.4 observed by (Shumway, 1960) owing to the assumption that the sediments have zero rigidity, which is invalid for marine sediments (*Section 2.5.1).* The use of an exponent of 2 has been used to invert measurements of compressional wave attenuation coefficient to sediment type (LeBlanc *et al.*, 1992a). Compilations also observe "some evidence" for non-linear frequency dependence, with non-linear regions occurring between 10 to 100 kHz in sands and 1 to 10 kHz in silts (Kibblewhite, 1989). The variable frequency-dependence predicted by Biot-Stoll Theory which has been considered by a number of authors is discussed in *Section 2.5.2.*

Frequency (kHz)	Attenuation coefficient ($dB \cdot m^{-1}$)	Exponent *q*	Sediment type	Reference
3.5 - 100	1.5 - 55	1	Sands (compilation)	(Hamilton, 1987)
15 - 1500	N/a	1	Silt/clay (reconstituted)	(McLeroy and DeLoach, 1968)
4 - 50	0.28 – 3.00	1 $\pm$ 15 %	Mud *(in situ)*	(Wood and Weston, 1964)
0.04 – 0.09	0.59	1	Clayey silt (remote)	(Bennett, 1967)
5 - 50	0.30 – 1.86	1	Silty clay *(in situ)*	(Lewis, 1971)
5 – 50	N/a	1.00 -1.26	Sand *(in situ)*	(McCann and McCann, 1969)
3.5 – 100.0	0.6 – 74.3	0.94 – 1.1	sand to clay *(in situ)*	(Hamilton, 1972)
20 - 40	0.10 –2.48	0.6 – 3.4	Sand to clayey silt (core samples)	(Shumway, 1960)
0.05 – 0.60	$5.6 \cdot 10^{-4}$ – $9.5 \cdot 10^{-3}$	1.01, 1.14	sand to silty clay (*in situ)*	(Rodgers *et al.*, 1993)
100 - 1000	40 - 150	1.3 – 2.0	Silt and clay (core samples)	(Courtney and Mayer, 1993b)
0.05 – 1.00	$2.2 \cdot 10^{-4}$ – $9.5 \cdot 10^{-4}$	1.25 – 1.50	N/a	(Evans and Carey, 1998)
0.2 – 1.5 200 - 800	1.0 – 3.7	0.63 0.88	Silts: (*in situ*) (laboratory)	(Best *et al.*, 2001)
0.03 - 500	$5.6 \cdot 10^{-4}$ - 90	1.12	muds (compilation)	(Bowles, 1997)
25 - 100	8 - 60	Non-linear	*S*and (*in situ)*	(Buckingham and Richardson, 2002)
20 - 300	3 - 34	Non-linear	Glass beads (laboratory)	(Hovem and Ingram, 1979)
0.125 - 400	1 - 200	Non-linear	sand *(in situ)*	(Williams *et al.*, 2002)

Table 2.2. Summary of measurement of compressional wave attenuation coefficients which span a range of frequencies.

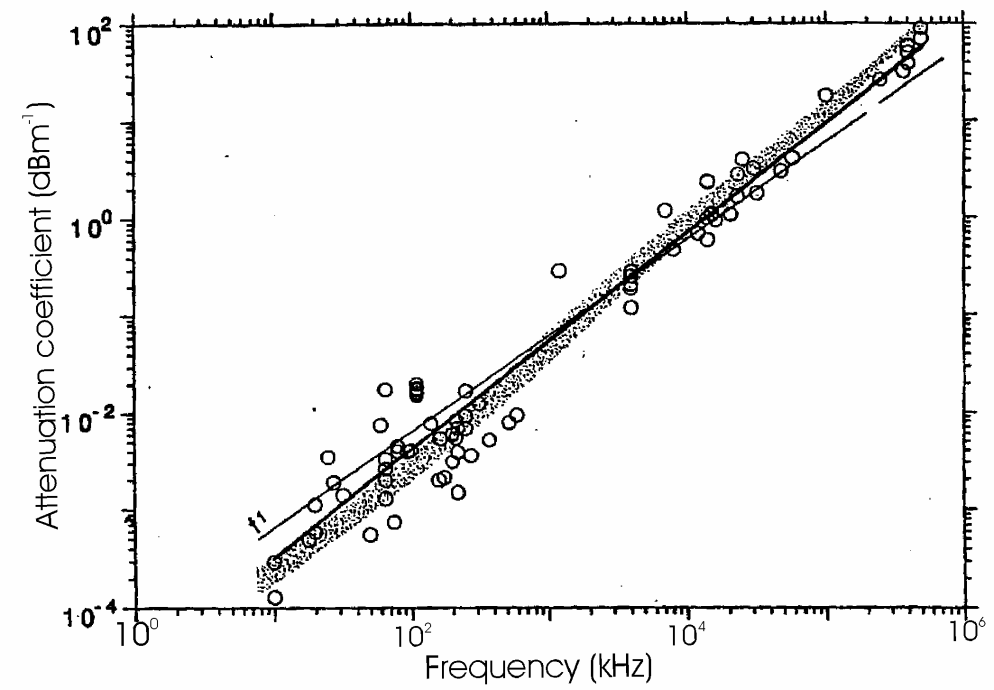

Figure 2.6. Compilation of attenuation coefficients from fine-grained sediments (denoted by circles), with linear relationship denoted as narrow line, $f^{1.12}$ relationship denoted by dark line and predictions from Biot-Stoll model denoted by shaded area. From (Bowles, 1997).

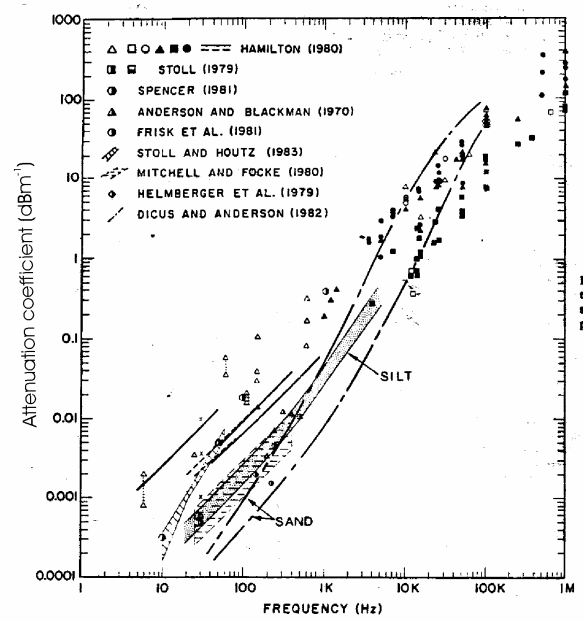

Figure 2.7. Addition of low frequency attenuation coefficients to Hamilton's compilation, from (Stoll, 1974). Predicted absorption coefficients from Biot-Stoll model are include for silts (shaded area) and sands (extremes displayed by dashed lines), with frequency-dependency observed by individual authors also included.

Additional research measures the quality factor of saturated marine sediments over a range of frequencies. Quality factor is observed to vary from 13 to 20, which remain constant within errors of approximately $\pm$ 3 to $\pm$ 6, in silts over the frequency range of 200 to 800 kHz (Best *et al.*, 2001). *In situ* measurements of quality factors in sands include values from 10 to 50 at frequencies of 1 to 30 kHz (Turgut and Yamamoto, 1990) and values from 28 to 500 for 3 to 80 kHz (Simpson *et al.*, 2003). The significance of respective peaks in quality factor at 4 kHz (Turgut and Yamamoto, 1990) and 6 kHz (Simpson *et al.*, 2003) are reduced due to a lack of published error analysis. Laboratory measurements of dry and saturated sands and silts made from 1 Hz to 1.5 kHz (Stoll, 1979) support a quality factor which is independent of frequency in dry sediments and decreases as frequency increases in saturated sediments.

Hence, though a linear relation between attenuation coefficient and frequency appears to adequately describe the general behaviour of marine sediments, more recent work implies that finer scale non-linear variations may be present. However, the absence of necessary error analysis in published literature and the intrinsic scatter of attenuation coefficients in sediment prevents either relationship from being confirmed.

2.4. Dependence of compressional wave properties on geotechnical properties

2.4.1. Dependence of velocity on geotechnical properties

The majority of the literature states that porosity is the dominant geotechnical factor which affects velocity (Hamilton, 1970; Horn *et al.*, 1968; Shumway, 1960), due to significant difference between the compressibility of the pore water and the sediment frame (Hamilton, 1971a). Velocity varies with porosity in a quadratic manner, decreasing as porosity increases from approximately 30 to 75 % and either remaining constant within errors and scatter, or increasing, as porosity increases above approximately 75 %, (Bachman and Hamilton, 1976; Courtney and Mayer, 1993b; Hamilton, 1970; Hamilton and Bachman, 1982; Horn *et al.*, 1968; Kim *et al.*, 2001; Orsi and Dunn, 1990; Orsi and Dunn, 1991; Richardson and Briggs, 1993; Richardson *et al.*, 1997). A typical example is displayed in *Figure 2.8.* Alternative linear and power relationships observed by additional authors are omitted due to the limited porosity range which they span, *i.e.* 8 % to 48 % (Endo, 1997) and 42 % to 74 % (Sutton *et al.*, 1957).

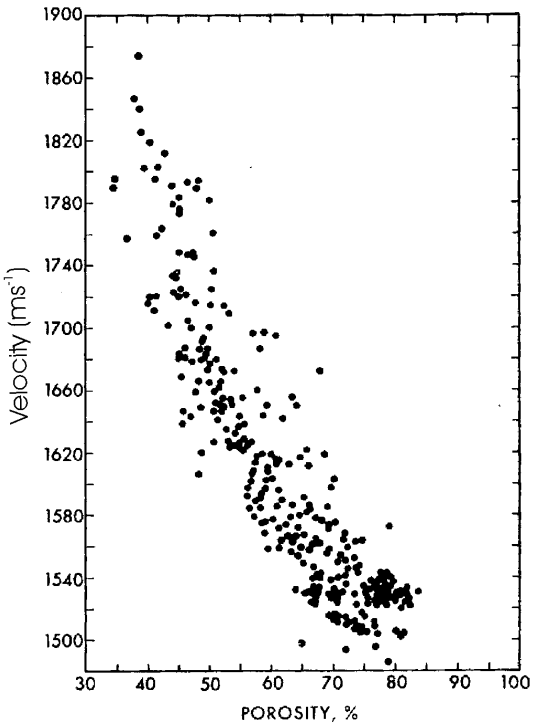

Figure 2.8. Compressional wave velocity versus porosity for continental shelf sediment for frequencies of 3.5 to 200 kHz. From (Hamilton, 1987).

The porosity at which the inflexion point occurs depends on the sedimentary environment under examination, ranging from 75% (Courtney and Mayer, 1993a), to 88 % (Hamilton, 1970). The increase in velocity at higher porosities is attributed to higher shear moduli at these porosities. These arise from a complex interaction of Van-der-Waals and coulombic forces, and cementation effects which arise from the redeposition of minerals (*e.g.* iron, manganese and phillipsite) from pore water onto mineral grains (Hamilton, 1970). Sediments with porosities greater than 70 % possess velocities less than that of pore water (Fry and Riatt, 1961; Hamilton, 1970; Hamilton, 1971a; Kim *et al.*, 2001; Nafe and Drake, 1963; Orsi and Dunn, 1990; Richardson and Briggs, 1993; Richardson *et al.*, 1997; Shumway, 1960; Sutton *et al.*, 1957). This is attributed to a balance between water and mineral compressibilities and densities, plus the effects of low rigidities and low mineral frame bulk moduli (Hamilton, 1971a).

In examining the relationships between velocity and porosity, the non-uniqueness of sediment should be considered. Hence, a single value of porosity can correspond to a variety of sediment types with a range of additional properties, *e.g.* a range of bulk densities, elastic moduli and mean grain diameters. Though porosity is identified as the

dominant property affecting velocity, these additional geotechnical properties have some effect which introduces a degree of variability into the velocity for a single porosity, *Figure 2.8*.

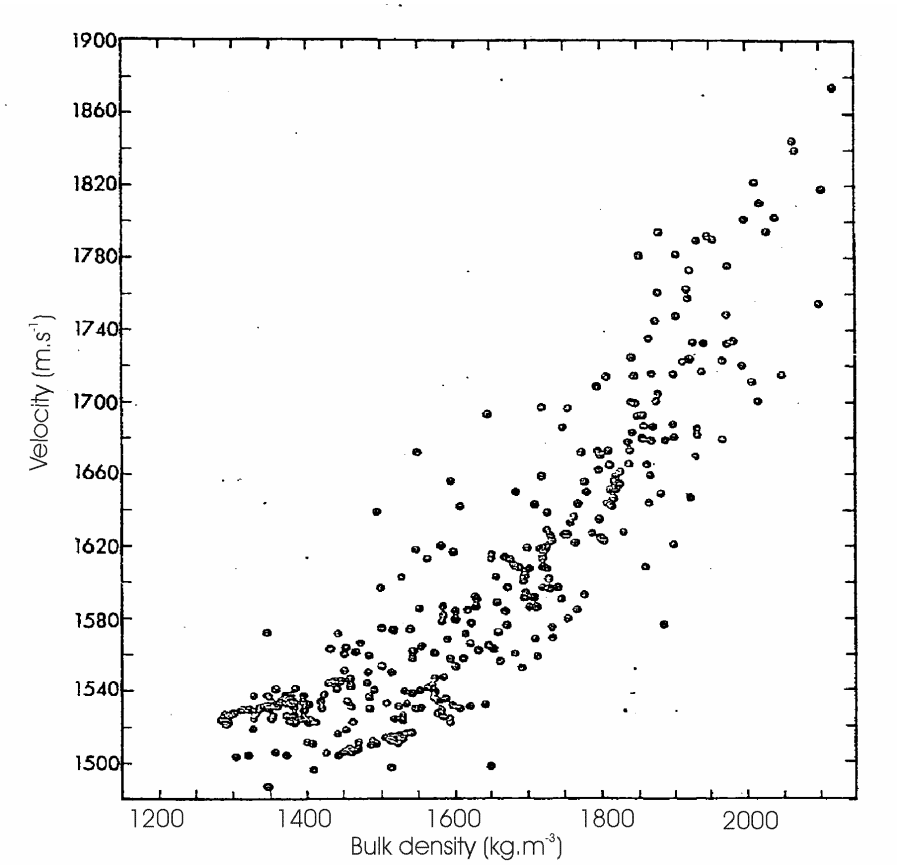

Figure 2.9. Compressional wave velocity versus bulk density for continental shelf sediments for frequencies of 3.5 to 200.0 kHz. From (Hamilton and Bachman, 1982).

As *Equation 2.10* and *Figure 2.4* display, bulk density decreases in a linear manner as porosity increases. Hence the relationship between velocity and density is a "mirror" image of the relationship between velocity and porosity, *Figure 2.8* versus *Figure 2.9.* Velocity is related to density in a quadratic manner with velocity decreasing, or remaining constant, as density increases up to approximately 1400 $kg \cdot m^{-3}$, and velocity increasing with density thereafter (Bachman, 1985; Gorgas *et al.*, 2002; Hamilton, 1970; Horn *et al.*, 1968; Orsi and Dunn, 1991; Richardson and Briggs, 1993; Richardson *et al.*, 1997). As in the case of porosity the inflexion varies with the sedimentary environment examined, ranging from 1165 $kg \cdot m^{-3}$ in sand-silt-clay to silty clay (Orsi and Dunn, 1991) to 1445 $kg \cdot m^{-3}$ in clayey-silt to clay (Orsi and Dunn, 1990). The linear relation between velocity

and density, which is presented by (Brandes *et al.*, 2001) is deemed unreliable due to the limited density range spanned, *i.e.* 1770 to 2060 $kg \cdot m^{-3}$.

The relationship between velocity and grain size parameters are also important, as grain size parameters are not affected by storage and drying and are standard geotechnical properties measured. Velocity increases with mean grain diameter, *Figure 2.10*, with a quadratic relationship favoured (Bachman, 1985; Horn *et al.*, 1968; Kim *et al.*, 2001; Orsi and Dunn, 1991; Richardson and Briggs, 1993). Typical velocities decrease from values greater than 1600 $m \cdot s^{-1}$ in sands (0 to 4 ϕ) to less than 1540 $m \cdot s^{-1}$ in clays (greater than 9 ϕ). Though the relationship between velocity and mean grain diameter is predominantly due to underlying changes in porosity, additional factors which are intrinsically related to grain size, e.g. the number of contacts and the frame moduli, will also have some effect.

The relationship between velocity and additional textural properties such as percentage of clay or sand sized particles are also examined by a number of authors. Velocity increases as percentage of sand sized particles increases (Hamilton, 1970; Lu *et al.*, 1998a) and percentage of clay sized particles decreases (Hamilton, 1970; Kim *et al.*, 2001; Orsi and Dunn, 1991). The relationship between percentage clay size particles and the velocity of artificial sediments is discussed in *Section 2.5.3*. No relationship is observed between velocity and additional grain size parameters, such as sorting, skewness and kurtosis (Horn *et al.*, 1968; Sutton *et al.*, 1957), except the increase in scatter as sorting becomes poorer. This scatter may be significant given the poorly sorted nature of many marine sediments.

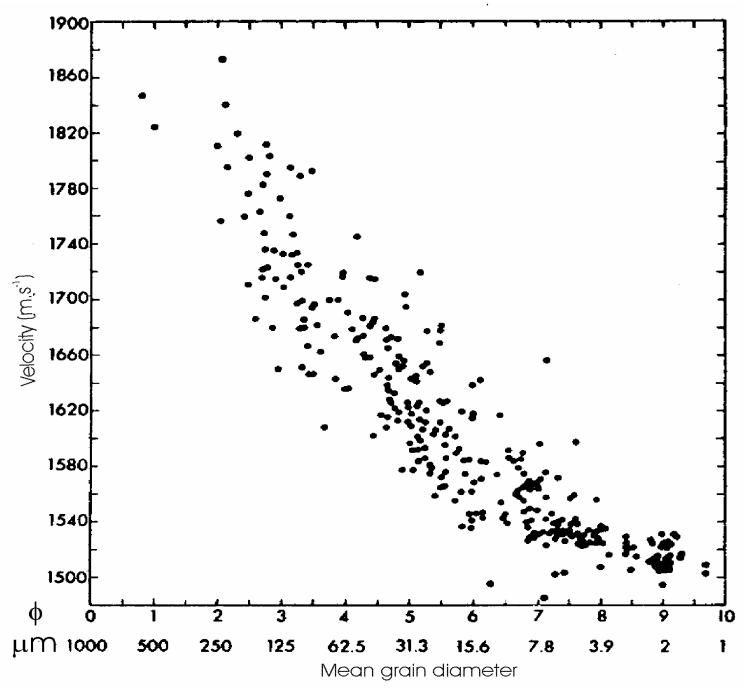

Figure 2.10. Compressional wave velocity versus mean grain diameter, in units of ϕ and μm, in continental shelf sediments at frequencies of 3.5 to 200 kHz. From (Hamilton, 1987).

Velocity also depends on the mineralogy, with minimum velocities observed in calcerous oozes (Fry and Riatt, 1961), velocity observe to increase with calcium carbonate content (Sutton *et al.*, 1957) and significantly different empirical relationships between velocity and geotechnical properties observed in siliclastic and carbonate sediments (Richardson *et al.*, 1997). The uniqueness of real sediments is highlighted by Brandes *et al* (Brandes *et al.*, 2001), who observed greater velocities for *in situ* sediment than well-sorted reconstituted samples, a consequence of increased grain-to-grain contacts in natural sediments which increases shear modulus.

A large number of authors have developed single empirical relationships which can be used to predict velocity from either porosity, density or mean grain diameter (Bachman, 1985; Brandes *et al.*, 2001; Courtney and Mayer, 1993b; Endo, 1997; Hamilton, 1970; Hamilton and Bachman, 1982; Kim *et al.*, 2001; Orsi and Dunn, 1990; Orsi and Dunn, 1991). Some authors produce multi-variable relationships, which use a single equation to relate velocity to a number of geotechnical properties (Lu *et al.*, 1998a; Sutton *et al.*, 1957).

It is debatable which geotechnical property or combination of geotechnical properties will result in the most accurate and reliable predictions of velocity. Orsi and Dunn (1990, 1991) state that porosity, bulk density, mean grain diameter and percentage of clay sized particles all result in a similar quality of velocity prediction, with errors of approximately $\pm$ 18 $m \cdot s^{-1}$, while percentage of sand sized particles produces the worst predictions, with no explicit errors quoted. Alternative authors state that mean grain diameter and percentage of clay sized particles are the best indices from which to predict velocity, resulting in errors less than $\pm$ 12 $m \cdot s^{-1}$, while the use of porosity or density result in errors of $\pm$ 29 $m \cdot s^{-1}$ (Hamilton and Bachman, 1982; Hamilton *et al.*, 1970).

The optimium empirical relationships between velocity and geotechnical properties are displayed in *Table 2.3.* (Richardson and Briggs, 1993). These have been selected due to the large range of geotechnical properties spanned and the examination of samples from a wide range of global sedimentary environments. For the large number of samples examined, *i.e.* 211 samples, goodness of fit (R^2) values greater than 0.82 denote a good fit to the data, with the higher values of R^2 for bulk density and porosity indicating the better estimates of velocity obtained from these properties than for mean grain diameter.

Independent variable	Regression equation	Valid range	R^2
M (ϕ)	$v=v_w \cdot (1.18 - 0.034 \cdot M + 0.0013 \cdot M^2)$	0 - 12 ϕ,	0.820
n (%)	$v=v_w \cdot (1.574 - 0.015 \cdot n + 0.0001 \cdot n^2)$	34 - 91 %	0.954
ρ ($g \cdot cm^{-3}$)	$v=v_w \cdot (1.623 - 0.936 \cdot \rho + 0.3417. \cdot \rho^2)$	1.17 – 2.1 $g \cdot cm^{-3}$	0.944

Table 2.3. Empirical relationships between velocity v and mean grain size M, porosity n and bulk density ρ. The velocity of water is represented by v_w while densities can be easily converted from $kg \cdot m^{-3}$ to $g \cdot cm^{-3}$ by dividing by a factor of 1000. From (Richardson and Briggs, 1993).

2.4.2. Dependence of attenuation coefficient and quality factor on geotechnical properties

Published literature concerning empirical relationships between attenuation coefficient and the geotechnical properties of sediments is relatively limited in comparison to the case for velocity. The geotechnical property with which attenuation coefficients have been most frequently compared is mean grain diameter. Attenuation coefficients, measured over a frequency range of 20 to 37 kHz, increase with mean grain diameter from 10 ϕ to 4 ϕ, and decreases as mean grain diameter increases from 4 to 1 ϕ (Shumway, 1960). This is displayed in *Figure 2.11*, with typical values ranging from 6 to 24 $dB \cdot m^{-1}$ for sands (M<4 ϕ), lying less than 24 $dB \cdot m^{-1}$ in silts (M from 4 to 9 ϕ) and less than 4 $dB \cdot m^{-1}$ in clays (M> 9 ϕ). The observed trend is attributed to the more well-sorted, homogeneous nature of the end member sediment types, with more heterogeneous sediment existing for mean grain diameters of approximately 4 ϕ (Stevenson *et al.*, 2002), owing to more equal proportions of non-surface active particles (sands and silts) and clay particles. The increased attenuation for these intermediate grain diameters arises from either increased scatter from heterogeneities or increased squirt flow (Best *et al.*, 2001). The spread of attenuation coefficients at each mean grain diameter is attributed to the non-uniqueness of sediment and variations in additional geotechnical properties.

Additional datasets which span more restricted ranges confirm these relationships (Brandes *et al.*, 2001; McCann and McCann, 1969). Attenuation coefficient also increases with the percentage of gravel (Briggs and Richardson, 1997) and increases as mud-to-sand ratio decreases (Best *et al.*, 2001). The increase in attenuation coefficient as sediments become coarser is either attributed to increased scatter of acoustic energy (Brandes *et al.*, 2001; Briggs and Richardson, 1997) or the increase in viscous losses (Best *et al.*, 2001). In well-sorted sediments permeability, and so global flow and viscous losses, increase as mean grain diameter increases (McCann and McCann, 1969).

Finally a number of authors observe a general increase in attenuation coefficient as the presence of scattering heterogeneities, e.g. shells and burrows (Gorgas *et al.*, 2002; Richardson and Briggs, 1993). An additional examination of the dependence of attenuation coefficient on geotechnical properties, which assumes a linear relationship between attenuation coefficient and frequency, is discussed in *Section 2.5.1* (Hamilton, 1972; Hamilton, 1987).

The dependence of attenuation coefficient on porosity has also been examined, with attenuation coefficient peaking at intermediate porosities of 45 to 60 % (Shumway, 1960). Details of published empirical relationships between attenuation coefficient and geotechnical properties are omitted from this thesis, owing to the considerable scatter in measured attenuation coefficients from identified relationships (Richardson *et al.*, 1997).

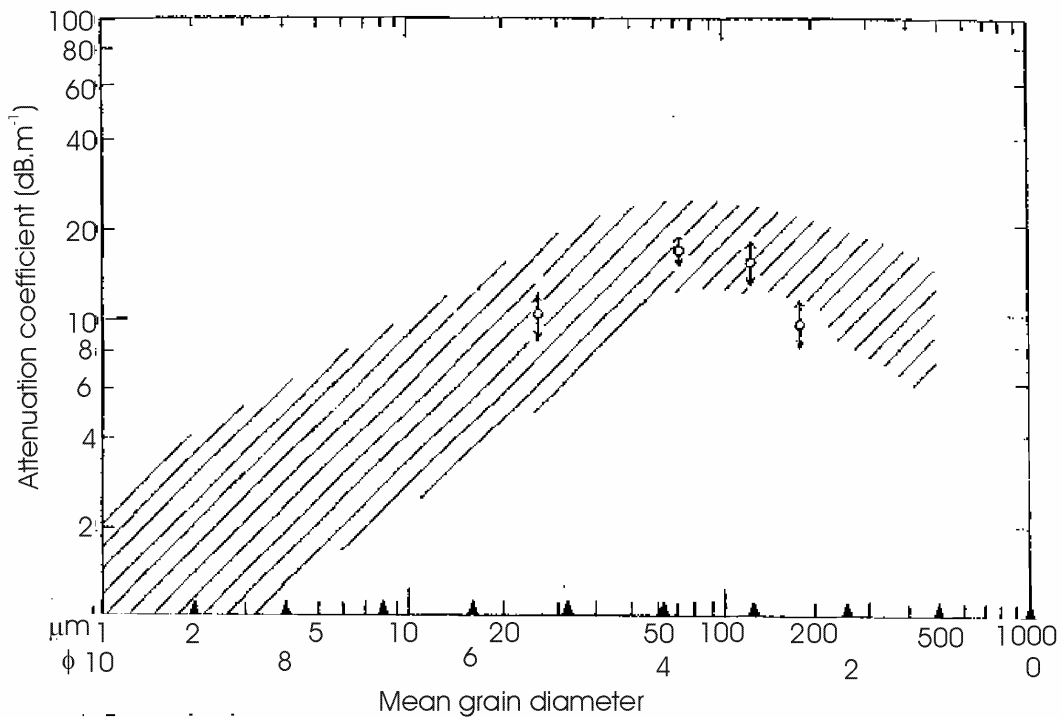

Figure 2.11. Attenuation coefficient versus mean grain diameter, with shaded area denoting measurements on laboratory samples over a frequency range of 20 to 37 kHz (Shumway, 1960) and circles denoting in situ measurements (McCann and McCann, 1969). From (McCann and McCann, 1969).

The dependence of quality factor on mean grain diameter has been examined by a limited number of authors, which include:

- Quality factors of 29 to 437 in coarse sands to clayey silts (with no errors stated) over a frequency range of 14 to 100 kHz (Hamilton, 1972).
- Quality factors of 14 to 58 in very coarse sands to very fine silts (with errors up to $\pm$ 19) over a frequency range of 1.5 to 12.5 kHz (Stevenson *et al.*, 2002).
- Quality factors of 7 to 910 in sands to silts (with errors from $\pm$ 3.7 to $\pm$ 92.9 %) over a frequency range of 5 to 20 kHz (Frazer and Fu, 1999).

The most thorough compilation of quality factors to date (Stevenson *et al.*, 2002) combines values from the first two sources in the above list with quality factors computed from laboratory measurements of velocity and attenuation coefficient (Shumway, 1960), *Figure 2.12.* Despite the considerable degree of scatter is present, quality factor increases as means grain diameter decreases from 4 to 10 ϕ, with no relationship clear within scatter for mean grain diameters less than 4 ϕ. This agrees with the decrease in attenuation coefficient as mean grain diameter decreases from 4 to 10 ϕ displayed in *Figure 2.11.*

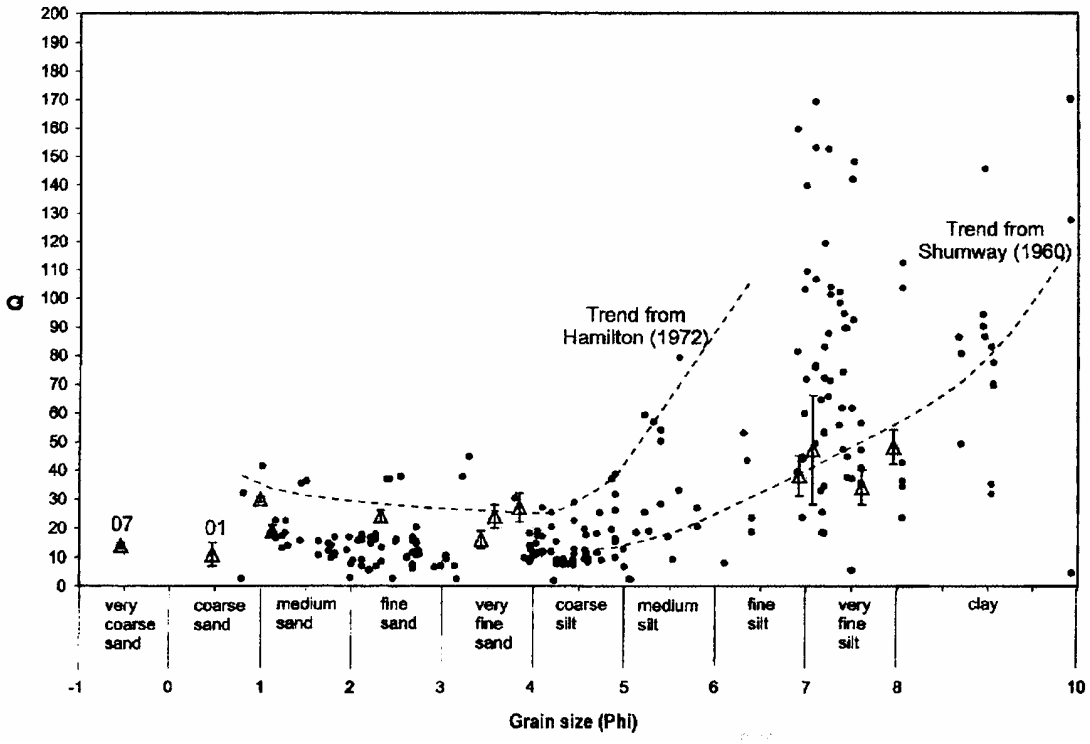

Figure 2.12. Dependence of quality factor on mean grain diameter including: measurements of quality factor both in situ (Hamilton, 1972) and on laboratory samples (Shumway, 1960), denoted by dots, empirical fits of previous two authors, denoted by dashed lines, and measurements of quality factor obtained from reflection data (Stevenson et al., 2002), denoted triangles with vertical error bars.

2.5. Geoacoustic models

A wide range of geoacoustic models exist, which adopt either purely theoretical or semi-empirical approaches. The following models have been omitted for the reasons stated:

- Hookean elastic models (Barkan, 1962) which are more relevant to the fields of soil mechanics and foundation engineering than sediment acoustics (Hamilton, 1971a; Hamilton, 1972).
- The Kelvin-Voigt model, which is rarely used due to its mathematical complexity.
- Scattering models, which are only applicable to marine sediments at frequencies greater than a "few" hundred kHz (Hamilton, 1971a). These frequencies are greater than those examined in this project, *Section 4.1*.
- Suspension models, which are not suitable owing to the finite rigidity of the majority of marine sediments (Hamilton, 1971a).
- Inter-granular shearing theory (Buckingham, 1998; Buckingham, 2000) considers the propagation of shear and compressional waves through marine sediment to be controlled by intergranular dissipation. This theory assumes that unconsolidated sediment possesses no skeletal frame and hence possesses an elastic rigidity of zero, which is invalid for the majority of sediment, see *Section 2.5.1*.

Only the three models most applicable to marine sediments are discussed below. Note that the velocities predicted by the models are phase velocities, while the loss mechanisms incorporated by the predicted energy losses depend on the model under consideration.

2.5.1. Linear viscoelastic model

A linear viscoelastic, or nearly elastic, model has been developed (Hamilton, 1971a; Hamilton, 1972). This is based on a semi-empirical approach which uses a combination of theory and measured moduli to predict phase velocity and an empirical fit to obtain attenuation coefficient. The model assumes that the quality factor and phase velocity are "virtually" independent of frequency, while attenuation coefficient, in $dB \cdot m^{-1}$, is "nearly" linearly related to frequency. The resulting model is stated to be valid for frequencies from "a few hertz to at least a few hundred kilohertz" (Hamilton, 1971a).

The linear viscoelastic model is derived from the basic equations of viscoelasticity (Ferry, 1961) in which the bulk modulus K and shear modulus μ have been replaced by complex moduli $(K+iK')$ and $(\mu+i\mu')$ respectively, where $i=(-1)^{1/2}$. In the case of small damping, *i.e.*$Q>10$ (see *Section 2.1*), the compressional wave phase velocity v can be calculated from

$$v = \left(\frac{K + \frac{4}{3}\mu}{\rho} \right)^{\frac{1}{2}} \qquad 2.12.$$

In the case of negligible shear modulus *Equation 2.12* condenses to Wood's Equation for a suspension (Wood, 1941),

$$v = \left(\frac{K}{\rho} \right)^{\frac{1}{2}} \qquad 2.13.$$

The finite rigidity of the majority of marine sediments has been confirmed, with some doubt still existing for sediments from estuaries, deltas and other areas with fast depositional rates (Hamilton, 1971a). This was achieved by comparing the product of the density and the phase velocity squared to the bulk modulus for a wide range of marine sediments, *Figure 2.13.* If these sediments possessed negligible shear modulus, the linear fit predicted by Wood's Equation should be applicable. The presence of data points above this line infer a finite shear modulus.

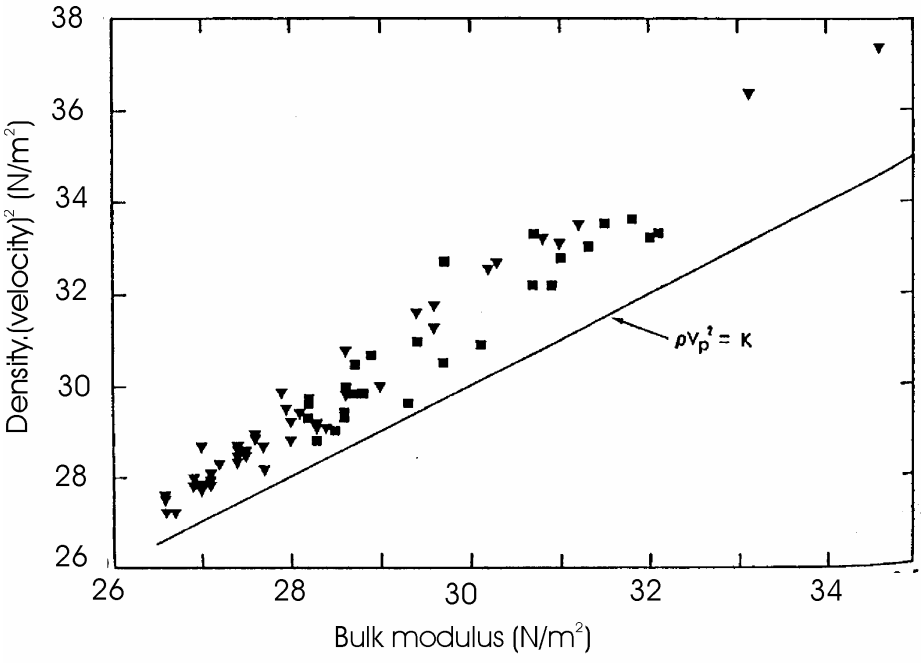

Figure 2.13. Comparison of the product of the density and the square of the velocity to bulk modulus for a range of marine sediments, including abyssal hill sediments (squares) and abyssal plain sediment (triangles). The predictions obtained from Wood's equation for suspensions are displayed. From (Hamilton, 1971a).

The bulk modulus can be obtained from the bulk moduli of the pore water K_f, bulk modulus of the mineral grains K_r and a frame modulus K_b using Gassmann's equations (Tuffin, 2001),

$$K = K_r \frac{K_b + Q_g}{K_r + Q_g} \qquad 2.14,$$

$$Q_g = \frac{100 \cdot K_f \cdot (K_r - K_b)}{n \cdot (K_r - K_f)} \qquad 2.15.$$

While the bulk moduli of pore water and mineral grains can be either measured or calculated from standard empirical equations, *Appendix A*, the manner of obtaining the frame bulk modulus is more complex. This involves the measurement of compressional and shear wave velocities and the use of *Equation 2.12* to obtain the bulk modulus of the sediment *K*. Knowledge of the porosity and bulk moduli of the pore water and mineral grains allows the frame bulk modulus to be computed from *Equations 2.14* and *2.15*. The frame bulk modulus decreases as porosity increases, due the reduced strength of the skeleton frame, *i.e.* the reduced number of grain-to-grain contacts as porosity increases. This combines with the highly compressible nature of water with respect to the mineral grains to produce a sediment bulk modulus *K* which decreases as porosity increases.

The shear modulus of the continuum depends on both the porosity and the angularity of the grains. Shear modulus decreases as porosity increases and angularity decreases. In clays, cohesional forces between particles dominate and the shear modulus decreases as the distance between the particles increases, *i.e.* as porosity increases. Though the dominant effect is sands is also that porosity, the affect of angularity of the grains is more pronounced than in clays, with increased angularity resulting in an increase in shear modulus.

The input parameters required to obtain compressional wave velocity from *Equation 2.12* can be determined in two ways. Firstly, the shear and bulk moduli and density of the sediment can be directly measured. Secondly, if only basic geotechnical information such as porosity or mean grain diameter is available, empirical relationships can be used to obtain the shear and frame bulk moduli. The frame bulk modulus is then combined with measured/calculated mineral and pore water bulk moduli, through *Equations 2.14* and *2.15,* to calculate the sediment bulk modulus. Concern is raised about

the use of the second method, due to the sparse nature of the data from which the empirical fits were derived.

Attenuation coefficient is obtained from the imaginary parts of the complex bulk and shear moduli (Hamilton, 1972). Under the assumption of "small-damping", attenuation coefficient is proportional to frequency and the approximate equation for quality factor, *Equation 2.8*, is valid. These factors will produce a quality factor which is independent of frequency. The attenuation coefficient obtained is expressed as

$$\alpha = k_h f \qquad 2.16,$$

where k_h will be termed Hamilton's parameter for the purposes of this thesis. This represents *Equation 2.11* for an exponent of unity. Hamilton's parameter incorporates all possible effects of the sediment structure, with values obtained by dividing attenuation coefficients available in pre-1971 literature by the relevant frequency. The empirical relationship between k_h and porosity is displayed in *Figure 2.14*.

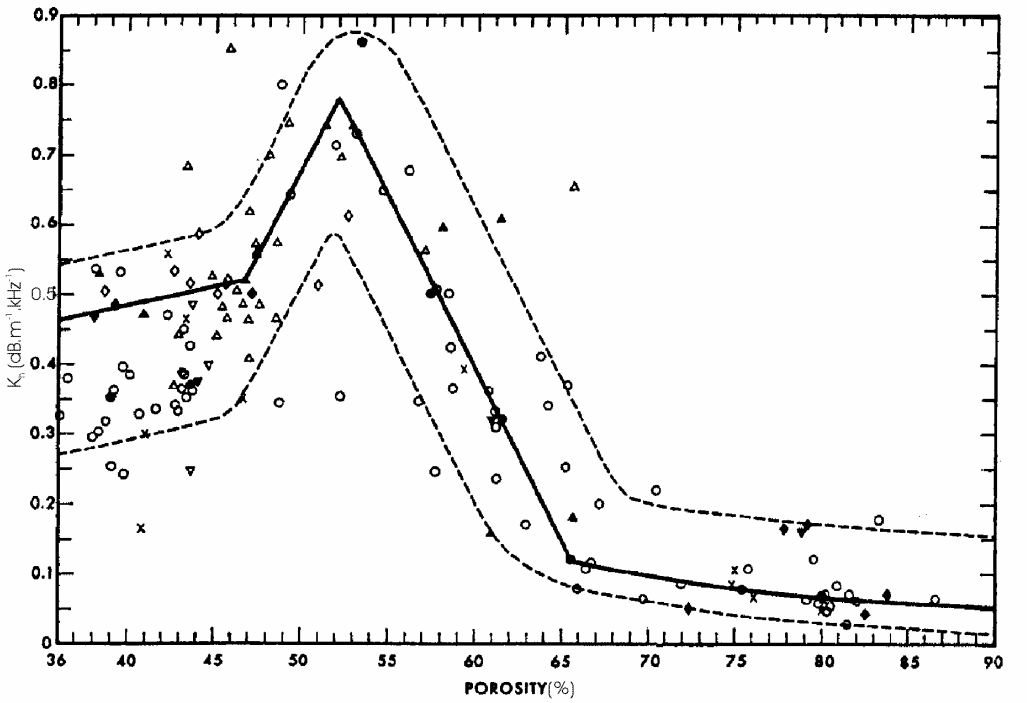

Figure 2.14. Variation of Hamilton's parameter k_h with porosity, with empirical fits applied by the author and relevant errors included. Symbols denote relevant literature sources from which k_h values have been obtained, details of which are available in the original paper (Hamilton, 1972).

Values of k_h range from 0.03 to 0.87 $dB \cdot m^{-1} \cdot kHz^{-1}$, with k_h increasing gradually with porosity from 36 to 47 %. From 47 to 52 % k_h increases more steeply, reaching a peak at 52 %. For porosities of 52 to 65 % k_h decreases with porosity to a value of approximately 0.1, whereafter k_h decreases gradually with porosity. This agrees with the dependence of attenuation coefficient on porosity observed by (Shumway, 1960).

In predominantly sandy sediments frictional forces dominate over interparticle forces. Hamilton (1971a) surmises that if frictional losses dominate, attenuation coefficients will depend primarily on changes in the surface area of grains that are in contact rather than changes in porosity. Computations indicate that, for coarse to medium sands, large changes in mean grain diameter result in small changes in porosity, while the discrepancy between the increase in porosity and grain-surface is more pronounced for fine sands to very fine silts (Shumway and Igelman, 1960). Hamilton re-examined the variations of k_h with porosity, and concluded that these variations fit better with the changes in contact areas than porosity and so frictional losses dominate.

In mixed sediments a combination of interparticle forces and frictional forces exist between the particles. Hamilton (1971a) again explained observed variations in k_h with porosity through frictional losses and contact areas. Increases in porosity signify the inclusion of more clay particles which force the larger sand and silt particles further apart. This reduces the number of grain-to-grain contacts of the coarser particles and so frictional losses decrease. The inflexion at approximately a porosity of 65 %, indicates the point at which all larger particles are suspended in the clay matrix and are no longer in contact, with much weaker inter-particle forces dominating at higher porosities. A similar porosity value at which all larger particles become separated was identified by (McCann and McCann, 1969).

Hence Hamilton concludes that “internal friction is by far the dominant dissipative process in water-saturated sediments. However, issues exist with the compilation dataset used to derive the linear visco-elastic model. The lack of a theoretical manner in which k_h can be calculated for a particular sediment type is disconcerting, while the large degree of scatter, especially about the peak value, results in the large error bars in the empirical fit, *Figure 2.14.*

2.5.2. Biot Theory

Biot Theory represents the accepted geoacoustic base model for marine sediment. It considers the macroscopic behaviour of wave propagation in saturated porous media (Biot, 1956b; Biot, 1956a), with the elastic constants used in the original theory converted into more accessible variables by later researchers (Geertsma and Smit, 1961). Biot considered a two-phase porous medium consisting of a pore fluid and a solid frame. In order to incorporate deviations from Poiseuille flow, which occur at frequencies greater than 10 Hz (Stoll, 1974), the viscous resistance to fluid flow is considered to be frequency dependent. Examination of elastic stresses and strains on the pore fluid and frame, under the assumption that the dissipation of acoustic energy is purely due to viscous forces which arise from the global motion of the pore fluid relative to the solid frame, allow coupled partial differential wave equations to be derived. As energy losses are limited to global viscous losses only, Biot Theory will predict an absorption coefficient, *i.e.* energy loss due to viscous losses only, rather than an attenuation coefficient, which includes interface and scattering losses. Two sets of coupled equations exist, one for shear and one for compressional waves, with the set for compressional waves as follows,

$$\nabla^2\left(P_b \cdot e + Q_b \cdot \varepsilon\right) = \frac{\partial^2}{\partial t^2}(\rho_{11} \cdot e + \rho_{12} \cdot \varepsilon) + b\frac{\partial}{\partial t}\left(e - \varepsilon\right) \qquad 2.17,$$

$$\nabla^2\left(Q_b \cdot e + R_b \cdot \varepsilon\right) = \frac{\partial^2}{\partial t^2}(\rho_{12} \cdot e + \rho_{22} \cdot \varepsilon) - b\frac{\partial}{\partial t}\left(e - \varepsilon\right) \qquad 2.18,$$

where e is the volume strain in the solid frame, ε is the volume strain in the fluid, Q_b is a measures of coupling between the volume change in the solid and that in the fluid, R_b is the pressure required to force a volume of fluid into the aggregate and ρ_{11}, ρ_{12} and ρ_{22} are coupled densities. P_b, Q_b and R_b are related to the porosity and elastic moduli of the sediment through *Equations 2.19* to *2.22* respectively, *i.e.*

$$P_b = \frac{K_r + K_b}{D - K_b} + K_b + \frac{4\mu}{3} \qquad 2.19,$$

$$Q_b = \frac{K_r\left(K_r - K_b\right)}{D - K_b} \qquad 2.20,$$

$$R_b = \frac{K_r^2}{D - K_r} \qquad 2.21,$$

$$D = K_r\left(1 + n\left(\frac{K_r}{K_f} - 1\right)\right) \qquad 2.22.$$

The coupled densities are obtained from the porosity and fluid and grain densities using

$$\rho_{11} = \left(1 - \frac{n}{100}\right)\cdot \rho_r + \rho_c \qquad 2.23,$$

$$\rho_{12} = -\rho_c \qquad 2.24,$$

$$\rho_{22} = \frac{n}{100}\cdot \rho_f + \rho_c \qquad 2.25,$$

with ρ_c denoting the mass coupling between the solid and the fluid (Best, 1992). This inertia term allows the effective mass of the solid and fluid to be coupled together and hence allow coupled wave propagation to be incorporated. Finally *b* represents the coefficient which controls the degree of energy damping which is obtained from

$$b = \frac{\eta\cdot(0.01\cdot n)^2}{k} \qquad 2.26,$$

where η represents fluid viscosity and *k* represent permeability.

The plane wave solutions of these equations predict one shear wave and two compressional waves, *i.e.* a fast and slow wave. The fast compressional wave represents the scenario where the frame and fluid are oscillating in phase and corresponds to disturbances generally observed in seismology (Best, 1992). The slow compressional wave represents the scenario when the frame and fluid are oscillating in antiphase, which results in considerable dissipation in water-saturated sediments and has only been observed in certain experimental studies (Johnston and Plona, 1982; Plona, 1980). Slow compressional waves are more dominant in media which contain more compressible pore fluids, such as gas, and may be relevant to gassy sediments (Gei and Carcione, 2003). The observation of the slow compressional wave in marine sediments is one of the strongest pieces of evidence supporting Biot Theory. The shear wave corresponds to the usual shear wave observed in seismology.

The Biot Theory results in phase velocities and absorption coefficients that depend on eleven geotechnical parameters and the frequency of the insonifying wave. The geotechnical properties can be considered in the following categories:

- the properties of the pore fluid, which include pore fluid density ρ_f, bulk modulus K_f and viscosity η.
- the properties of the mineral grains, which include mineral grain density ρ_r and bulk modulus K_r.
- the properties of the sediment frame, which include porosity n, shear modulus μ, frame bulk modulus K_b, permeability k, pore size parameter a and tortuosity γ.

Porosity, bulk density and bulk moduli have been previously discussed in *Sections 2.1* and *2.5.1*. The fluid viscosity η is the ratio of the shearing stress to the rate of strain in a fluid (Williams and Elder, 1989) and is a measure of the resistance to flow possessed by the fluid. The permeability k is defined from Darcy's law, which states that the flow of pore fluid through a sample of porous material is proportional to both the pressure difference across the sample and the cross sectional area of the sample and inversely related to the viscosity of the fluid and the length of the sample. The constant of proportionality is the permeability and hence the permeability measures the ability of fluid to pass through a porous media.

The tortuosity, or structure factor, is the sole property which is unique to the Biot model. The pore space in sediment will possess a multi-directional, tortuous nature. Hence less fluid will flow in and out of pores than for the case of uniform, cylindrical pores, which lie parallel to the pressure gradient exerted. The degree of flow reduction is controlled by the tortuosity. Theoretical values of tortuosity vary from 1, for uniform cylindrical pores parallel to the pressure gradient exerted, to 3, for a random system of uniform pores (Stoll, 1974).

The remainder of this discussion focuses on the fast compressional wave, as this corresponds to the wave typically observed in sediment acoustics. This displays a phase velocity which approaches a lower limit at low frequencies and a upper limit at high frequencies, and so displays a dispersive frequency region in between. The input geotechnical properties have variable effects on the resulting velocity, depending on their intrinsic significance to velocity and the range over which input values can vary in saturated marine sediments. Typical ranges have been obtained from relevant literature and are displayed in *Table 2.4*. Only values which have been directly related to sediment, *i.e.* those obtained from a direct measurement on a sediment sample or those which result in optimum fits of predicted velocities and absorption coefficients to measured values,

have been used. The range of grain bulk moduli used omit lower values measured under high stress-strain conditions (Molis and Chotiros, 1992), which are much lower than the dynamic bulk moduli required for acoustic modelling purposes (Richardson *et al.*, 2002).

Input property	Units	Range	References
ρ_f	$Kg \cdot m^{-3}$	*1000 - 1030*	*Min: (Stoll, 1985)* *Max: (Courtney and Mayer, 1993a)*
K_f	*GPa*	*2.00 – 2.42*	*Min: (Stoll, 1985)* *Max: (Williams et al., 2002)*
η	$Pa \cdot s$	*0.95 – 1.15*	*(Williams et al., 2002)*
ρ_r	$Kg \cdot m^{-3}$	*2650 - 2750*	*(Hamilton and Bachman, 1982)*
K_r	*GPa*	*32 – 49*	*(Williams et al., 2002)*
n	*%*	*35 – 90*	*(Richardson and Briggs, 1993)*
μ	*GPa*	*0.016 - 0.567*	*Min: (Williams et al., 2002)* *Max: (Stoll, 1979)*
K_b	*GPa*	*0.0012 - 11*	*Min: (Stoll, 1985)* *Max: (Hamilton, 1971a)*
k	m^2	$2.5x10^{-14} – 6.1x10^{-11}$	*Min: (Stoll, 1985)* *Max: (Williams et al., 2002)*
a	μm	*0.1 – 39*	*Min: (Stoll and Bautista, 1998)* *Max: (Stoll, 1977)*
γ	-	*1.15 – 1.71*	*Min: (Stoll, 2001)* *Max: (Wylie and Gregory, 1955)*

Table 2.4. Range of published Biot input parameters, which are relevant to saturated marine sediments. Note dimensionless nature of the tortuosity term γ.

The effect of each of input properties on predicted phase velocity was assessed from 300 Hz to 100 kHz through the use of software developed by (Best *et al.*, 2001) and the viable ranges for each input parameter, *Table 2.4,* with the results summarised in *Table 2.5*. This frequency range represents the region over which most frequency-dependent effects occur (Stoll and Bryan, 1970). Over the permitted ranges the properties which alter velocity by less than 1 % are deemed to have negligible effect. Velocity increases by a constant amount across all frequencies as the bulk moduli of the mineral grains and sediment frame increase and decreases by a constant amount as mineral grain density and porosity increase. As the tortuosity increases the high frequency (*i.e.* greater than 10 kHz) upper limit of velocity increases and the intermediate frequency range over which dispersion occurs increases as permeability and pore size increase.

Negligible effect (<1 % difference)	ρ_f K_f η μ
Frequency independent effect	K_r K_b ρ_r n
Affects high frequency only	γ
General frequency dependent effect	k a

Table 2.5. Effect of input Biot properties on fast compressional wave phase velocity.

The effects of properties that are frequency-dependent are displayed in *Figure 2.15*. These were evaluated using typical values of tortuosity, permeability and pore size for a fine sand, very fine sand and coarse silt, *Table 2.6.* The tortuosity was computed from typical porosities using an empirical relationship derived by (Berryman, 1980), see *Section 7.1.3* for details. This justifies the inclusion of porosity in the properties tested. It is pointless to examine the effects of each property independently owing to their interrelated nature

Sediment type	Fine sand	Very fine sand	Coarse silt
n (%)	*40*	*50*	*60*
k (m^2)	*$5x10^{-11}$*	*$1x10^{-11}$*	*$5x10^{-12}$*
a (μm)	*50*	*10*	*5*
γ	*1.75*	*1.5*	*1.33*

Table 2.6. Typical values of porosity n, permeability k, pore size parameter a and tortuosity γ used for fine sand, very fine sand and coarse silt.

As the porosity decreases, and so the sediment frame becomes more permeable and pore spaces become smaller and less tortuous, the overall magnitude of the velocity decreases. Both the range of frequencies and magnitude of the frequencies over which the transitional dispersion effects occur decreases as the sediment frame becomes less porous, with this transitional range existing for frequencies greater than 100 kHz in fine sands. Note that over the frequencies examined within this project, i.e. 16 to 100 kHz (Section 4.1) a dispersion of less than 1 % is predicted for all sediment types examined.

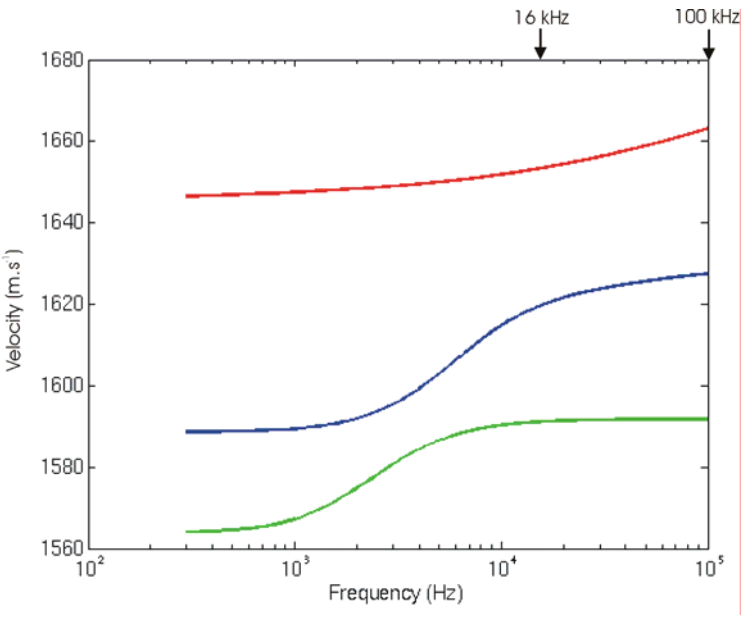

Figure 2.15. Predicted phase velocity of fast compressional wave for fine sand (red), very fine sand (blue) and coarse silt (green), with frequency range of project marked.

The absorption coefficient of the fast compressional wave varies in a non-linear manner with frequency. At low frequencies attenuation coefficient varies with f^2, while at high frequencies a $f^{1/2}$ dependence exists, with the definition of "high" and "low" frequency dependent on sediment type. The effect of each input property was considered, as described for velocity, and summaries drawn in *Table 2.7.*

Negligible effect (< 2.5 % difference)	ρ_f K_f K_r K_b μ
Affects high frequency only	γ η ρ_r n
General frequency dependent effect	k a

Table 2.7. Effect of input Biot properties on fast compressional wave absorption coefficient.

Variations on the properties defined as having negligible effect alter absorption coefficient by less than 2.5 %. High frequency absorption coefficients increase as viscosity, grain density and porosity increase and decrease as tortuosity decreases. The transition frequency range over which the frequency dependence changes increases as both permeability and pore size increase. Typical absorption coefficients are computed for the sediments in *Table 2.6,* and displayed in *Figure 2.16*. As the sediment type becomes finer both the magnitude of the high frequency absorption coefficient and the frequency range over which the frequency relationship changes increase, with the inflexion in the curve occurring from 2 to 8 KHz in coarse silts, 5 to 10 kHz in very fine sands and greater than 100 kHz in fine sands.

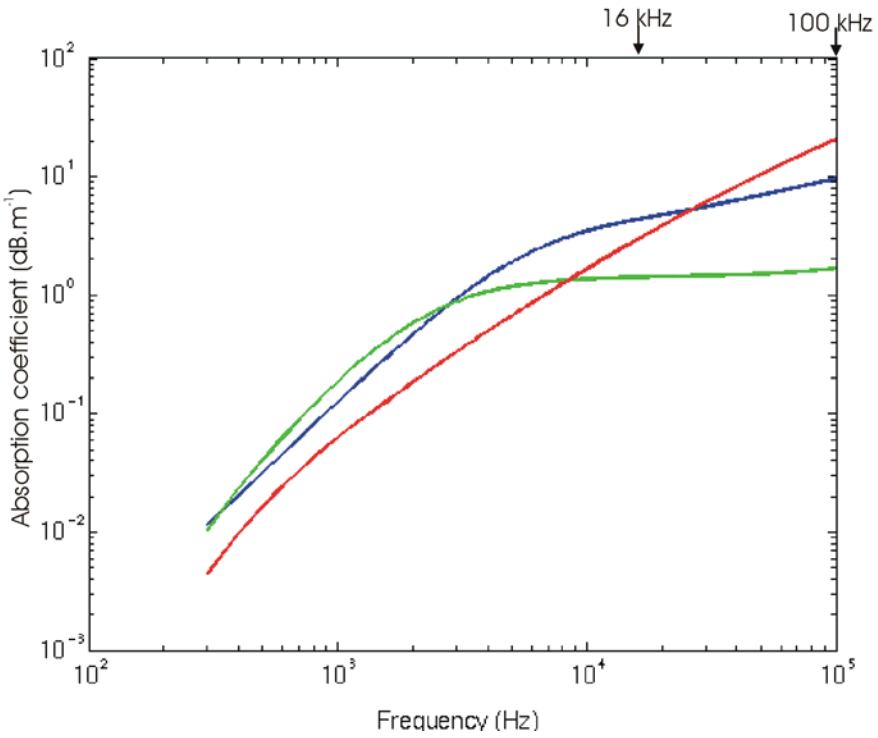

Figure 2.16. Predicted absorption coefficient of fast compressional wave for fine sand (red), very fine sand (blue) and coarse silt (green), with frequency range of present project marked.

Though the discussion to present has been limited to the original version of Biot Theory, this theory been modified by certain researchers. These modifications and the resulting theories will now be discussed. The Biot-Stoll Theory (Stoll, 1974) incorporates the inelasticity of the frame, *i.e.* frictional losses at grain-to-grain contacts in sands and local viscous losses (squirt flow) which occur in confined regions in silts and clays. This is achieved through complex, frequency-dependent terms for the bulk and shear moduli of the sediment frame. For coarse-grained sediments such inelastic effects will be important at frequencies less than a few Hz, while in fine-grained silts and clays limited global flow will allow squirt flow to dominate up to higher frequencies. Comparison of the Biot-Stoll and Biot theories for fine-grained sediment display that the Biot-Stoll theory predicts greater absorption coefficients which are proportional to frequency for a greater range of frequencies (Leurer, 1997). For fined grained sediments, Biot theory predicts absorption coefficients of 0.006 $dB \cdot m^{-1}$ at 16 kHz to 0.2 $dB \cdot m^{-1}$ at 100 kHz while Biot-Stoll theory predicts values of 0.25 and 2 $dB \cdot m^{-1}$ respectively (Leurer, 1997).

Velocities predicted by the Biot-Stoll Theory agree well with those measured in artificial sediment from 15 to 300 kHz (Hovem, 1980) and *in situ* sands from 125 Hz to

400 kHz (Buckingham and Richardson, 2002; Stoll, 2001; Turgut and Yamamoto, 1990; Williams *et al.*, 2002), *Figure 2.17*. Though measured and predicted velocities agree, concern is raised over the manner in which the Biot Theory was applied, which neglects the interrelated manner of the frame parameters. This accounts for the much greater degrees of dispersion than observed in *Figure 2.15*.

Typical absorption coefficients predicted by Biot-Stoll theory are displayed in *Figure 2.7* for sands and silts, which agree with the compilation of measured attenuation coefficients within the spread of values observed (Stoll, 1974). Individual projects report that attenuation coefficients measured in glass beads from 20 to 300 kHz (Hovem and Ingram, 1979) and sands from 1 to 400 kHz are well predicted by Biot-Stoll Theory (Stoll, 2001; Williams *et al.*, 2002). Alternative research finds predicted absorption coefficients to underestimate attenuation coefficients measured *in situ* in sands and silts from 10 Hz to 1 MHz (Best *et al.*, 2001; Buckingham and Richardson, 2002). This discrepancy is particularly pronounced at higher frequencies and is attributed to either scattering losses from heterogeneities in the sediment (Best *et al.*, 2001; Buckingham and Richardson, 2002; Williams *et al.*, 2002) or energy losses associated with shearing at grain contacts (Buckingham, 2000).

Further modifications have been applied to Biot-Stoll Theory to produce the effective grain model (EGM). This considers three types of sediment grains, namely sand or silt particles, non-swelling clay particles and swelling clay particles, with the distinction of the clay particles into swelling and non-swelling categories permitting increased squirt flow (Leurer, 1997). Absorption coefficients predicted by the EGM are greater than those predicted by Biot-Stoll Theory, while the frequency range over which absorption coefficient is proportional to frequency is reduced. Though the EGM provides a comparatively good fit to compressional wave properties measured in fine-grained sediment, "a reliable test of its capability can only be carried out by further experiments on physically well-described sediment samples" (Leurer, 1997). To date no such tests are available in the extant literature.

Alternatively adjustments to Biot-Stoll Theory allow a distribution of grain sizes to be incorporated (McCann and McCann, 1985), hence making it more applicable to natural sediments. Velocities and absorption coefficients predicted by this multiple pore model agree better with those measured in beach sands and glass beads from 15 to 300 kHz than

those obtained from the single pore model. The resulting theory allows viscous losses to produce absorption coefficients which are proportional to frequency and a quality factor which is independent of frequency in poorly sorted sediments.

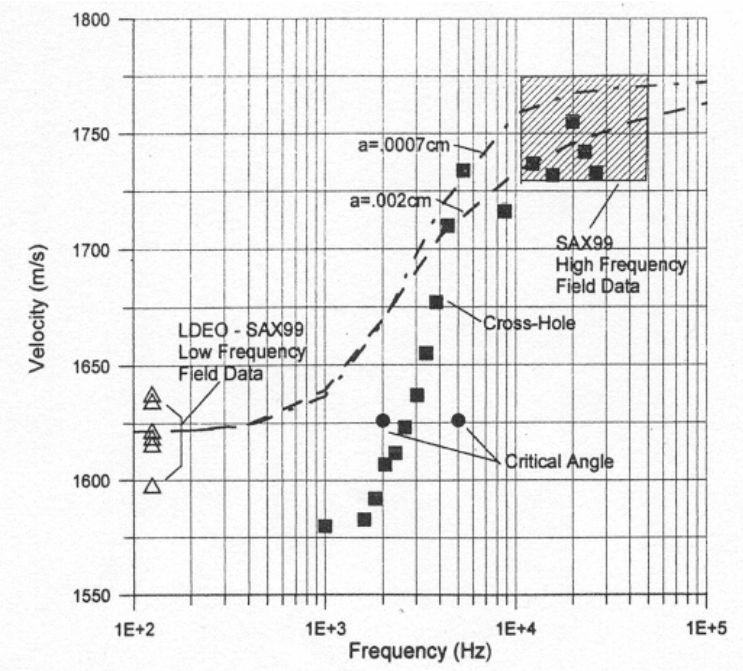

Figure 2.17. Comparison of measured compressional wave velocities (discrete symbols) to fast wave phase velocities predicted by Biot-Stoll Theory (dashed line) which were obtained using variable pore size parameters a. From (Stoll, 2001), which contains details of experimental techniques used to obtain measured velocities.

2.5.3. Micro-geometrical model

A micro-geometrical model has been developed which relates compressional wave phase velocity to the percentage of clay sized particles (Marion *et al.*, 1992; Nur *et al.*, 1991). This attributes the scatter in typical velocity versus porosity plots, *Figure 2.8,* to variations in the percentage of clay size material. The micro-geometrical model has been derived from measurements of compressional wave velocity in artificial sediments, which consist of well-rounded, well-sorted quartz grains (1.55 – 2.18 ϕ) and kaolinite clay (7.97 – 9.97 ϕ) at pressures ranging from 0 to 50 MPa. At room pressure porosity decreases as clay content increases from 0 to 20 % and increases with clay content thereafter, while velocity increases as clay content increases from 0 to 20 % and decreases as clay content increases thereafter. As pressure increases the critical clay content at which the porosity

minimum and velocity maximum occur also increases. The micro-geometrical model reflects these trends, *Figure 2.18,* through a detailed consideration of the sediment structure. For fractional clay contents less than the porosity of the pure sand, clay particles lie in pore spaces between sand particles. Hence the pore fluid is considered to be a mixture of clay and water, the bulk modulus of which can be determined from *Equations 2.14* and *2.15*. For clay fractions greater than the porosity of the pure sand the sand particles become suspended in a clay matrix, the bulk modulus of which is computed using the Reuss average.

Though this model describes the measured properties of the artificial sediments examined, is applicability to natural sediments has not yet been examined. Natural sediment will possess a broader range of grain sizes and less distinct end members. A decrease in velocity has been observed in natural marine sediments as clay content increases (Hamilton, 1970; Kim *et al.*, 2001; Orsi and Dunn, 1991), with a typical relationship displayed in *Figure 2.19*. Unfortunately the lack of published velocities for clay contents less than 20 % prevent the applicability of the micro-geometrical model to natural sediments being deduced. An additional limitation of the micro-geometrical model is the relatively high pressures at which experimental velocities have been recorded. These pressures corresponds to surficial sediments lying greater than 990m below the water surface, hence additional measurements at lower pressures are required to relate the micro-geometrical model to shallow marine sediments. Finally only velocity can be determined, while the previously discussed linear visco-elastic model and Biot Theory allow both velocity and attenuation/absorption coefficient to be determined.

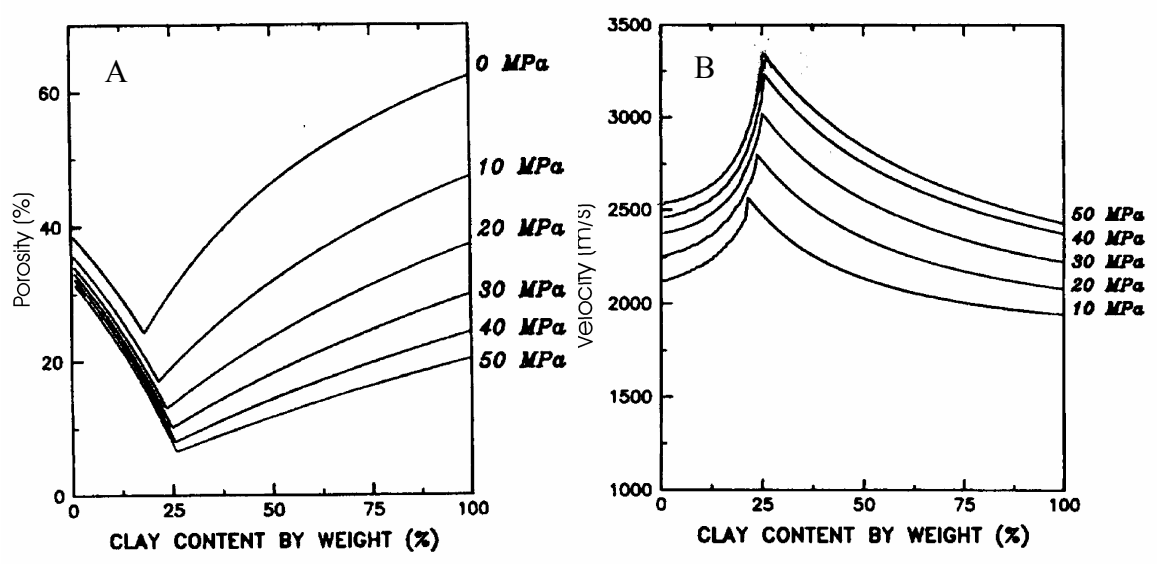

Figure 2.18. Porosity (A) and compressional wave phase velocity (B) predicted by micro-geometrical model, from (Marion et al., 1992).

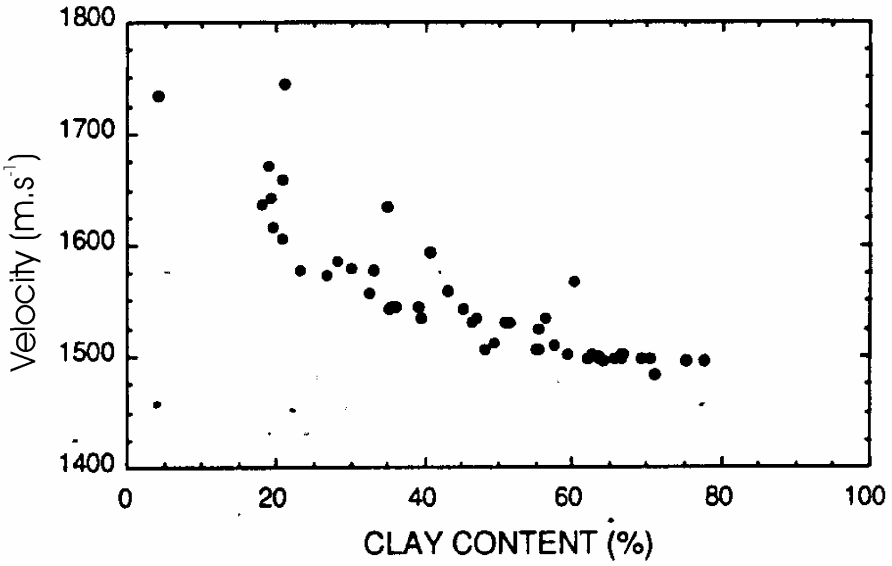

Figure 2.19. Relationship between compressional wave velocity and clay content observed in natural sediment at frequencies of 400 kHz, from (Orsi and Dunn, 1991).

2.5.4. Critique of attenuation mechanisms

In light of the previous discussion a final critique of energy loss mechanisms in marine sediments is necessary. The linear visco-elastic theory assumes that attenuation is due to frictional losses only, while Biot Theory incorporates global viscous losses only. Alternatively Biot-Stoll Theory incorporates energy loss from frictional, global viscous and local viscous sources.

If energy loss is dominated by frictional losses at grain-to-grain boundaries, the attenuation coefficient will depend on the strain amplitude of the acoustic waves (Cascante, 1996). However, for strains amplitudes less than 10^{-6}, *i.e.* those typically encountered using seismic techniques, attenuation coefficient is independent of strain amplitude (Johnston *et al.*, 1979; Murphy, 1984; Stoll, 1985; Winkler and Nur, 1978).

Examination of the attenuation coefficients and quality factors in rocks can give essential insights into sediments. In dry rocks it is accepted that attenuation coefficient is proportional to frequency and velocity and quality factor are independent of frequency over the frequency range of a few Hz to 100 kHz (Johnston *et al.*, 1979; Kibblewhite, 1989; Stoll, 1985). This implies that frictional losses at grain-to-grain contacts dominate in dry rocks (Johnston *et al.*, 1979; Stoll, 1974). The relationship in saturated rocks is much more complex, with a non-linear relationship observed between attenuation coefficient and frequency from 10 kHz to 100 kHz in wet sandstones (Kibblewhite, 1989), a quality factor that decreases as frequency increases from 73 to 638 kHz in wet sandstone (Murphy, 1984) and significant frequency-dependence in quality factor from 500 Hz to 1.7 kHz (Winkler and Plona, 1982). This frequency-dependent nature combines with the measurement of extremely large quality factors ($Q \leq 2000$) in out-gassed dried rocks (Tittmann, 1981) to confirm that viscous losses are the dominate mechanism in saturated rocks, with global flow dominating at low frequencies in more permeable rocks and local flow dominating in less permeable rocks at higher frequencies (Best and McCann, 1995; Johnston *et al.*, 1979; Winkler and Plona, 1982).

As frictional forces can be discounted as a significant source of energy dissipation in saturated rocks, which are much more consolidated and cemented than sediment, it is concluded that viscous losses dominate in saturated marine sediments. Though this invalidates the loss mechanisms considered in the linear-visco elastic theory, the empirical approach adopted may allow certain relationships obtained from this theory to remain valid.

Viscous losses can result in a range of relationships between predicted absorption coefficient and frequency, including f^2, $f^{1/2}$ *and* f^1. In high permeable sands it is hypothesised that global fluid motion occurs, while in less permeable silts and clays, local fluid motion may occur, with global flow only a factor at higher frequencies (Best *et al.*, 2001; Stoll, 1985). The frequency-dependence of absorption coefficients which arise from

viscous losses is difficult to ascertain, with a linear relationship dominating for certain versions of Biot theory (Biot-Stoll theory and the inclusion of a range of grain-size distributions) while f^2 and $f^{1/2}$ dependences dominate in alternative versions (original Biot theory and EGM).

2.6. Summary

Relationships between geotechnical properties are well understood, and have been related to typical sediment structures. Porosity is observed to increase as mean grain diameter decreases, due to the construction of more open structures and the presence of adsorbed water in fine-grained sediments. The limited range of sediment grains present in marine sediments results in porosity being the dominant factor which affects bulk density.

A wide suite of literature is available to support both dispersive and non-dispersive sediment, with the general lack of published error analysis preventing the confirmation of one choice. To a first order approximation attenuation coefficient is proportional to frequency, while quality factor is frequency-independent. Though additional low frequency datasets support a non-linear relationship, general oversights in research which examines the frequency-dependence of attenuation coefficient make it impossible to reliably distinguish between a linear or non-linear frequency-dependence. These include the use of compilations of attenuation coefficients, the scatter in attenuation coefficients and the apparent lack of sufficient error analysis.

The relationship between velocity and geotechnical properties of sediments have been well examined. Velocity is observed to depend on porosity, mean grain diameter and density in a quadratic manner, with velocity generally decreasing as porosity decreases, mean grain diameter increases and density increases. The scatter in the observed relationships signify that porosity is the dominant geotechnical property affecting velocity due to significant difference between the compressibility of the pore water and sediment frame. Relationships between attenuation coefficient and quality factor, and the geotechnical properties of sediments have been less rigorously examined. Attenuation coefficient is observed to vary in a quadratic manner with mean grain diameter, displaying a maximum value at approximately 4 ϕ.

Certain geoacoustic models are discussed which include:

- The linear visco-elastic model which predicts no velocity dispersion, an attenuation coefficient that is linearly related to frequency and dominated by frictional losses at grain-to-grain contacts and a quality factor which is frequency independent. Though this loss mechanism has been invalidated, the empirical approach adopted in the construction of this model may allow certain relationships derived to remain valid.
- Biot Theory which predicts the propagation of three waves; two compressional waves and one shear wave. The fast compressional wave corresponds to the wave typically observed in sediment acoustics and possesses a non-linear velocity dispersion and a non-linear relationship between attenuation coefficient and frequency. The dominant energy loss mechanism is viscous losses and a frequency-dependent quality factor is predicted. Modifications to the original Biot Theory include the addition of friction losses and squirt flow to produce the Biot-Stoll theory and the inclusion of a grain size distribution, which predicts an attenuation coefficient which is proportional to frequency.
- The micro-geometrical model, which relates velocity to clay content, predicts a velocity which peaks at 20 % clay content at atmospheric pressure. This cannot be validated in natural sediment due to the lack of published velocity at clay contents less than 20 % and the high pressures for which the model is obtained.

The independence of attenuation coefficient on strain amplitude and negligible effect of frictional losses in rocks both imply that viscous losses, on either a global or local scale, dominate in marine sediments.

References- will all be at end of thesis.

Bachman, R. T. and Hamilton, E. L., Density, Porosity, and grain size of samples from deep sea drilling project site 222 (leg 23) in the Arabian Sea *Journal of Sedimentary Petrology, 46 (3)*, 654-658, 1976

Bachman, R. T., Acoustic and physical property relationships in marine sediment *Journal of the Acoustic Society of America, 78 (2)*, 616-621, 1985

Barkan, D. D., Dynamics of bases and foundations, McGraw--Hill, Nwe York, 434 pp, 1962.

Bennett, L. C., In situ measurements of acoustic absorption in unconsolidated sediments (abstract only) *Transactions to the American Geophysical Union, 48*, 144, 1967

Berryman, J. G., Confirmation of Biot's theory *Applied Physics letters, 37*, 382-384, 1980

Best, A. I., The prediction of the reservoir properties of sedimentary rocks from seismic measurements, PhD, Postgraduate Institute of Sedimentology, University of Reading, 390 pp, 1992.

Best, A. I., The prediction of the reservoir properties of sediemntary rocks from seismic measurements, PhD, Department of Sedimentology, Reading, 390 pp, 1992.

Best, A. I. and McCann, C., Seismic attenuation and pore-fluid viscosity in clay-rich reservoir sandstones. *Geophysics, 60 (5)*, 1386-1397, 1995

Best, A. I., Huggett, Q. J. and Harris, A. J. K., Comparison of in situ and laboratory acoustic measurements on Lougth Hyne marine sediments *Journal of the Acoustic Society of America, 110 (2)*, 695-709, 2001

Biot, M. A., Theory of Propagation of Elastic Waves in Fluid-Saturated Porous Solids. 1. Low-Frequency Range. *Journal of the Acoustical Society of America, 28*, 168-178, 1956 (a).

Biot, M. A., The theory of propagation of elastic waves in a fluid-saturated porous solid. 2. Higher frequency range. *Journal of the Acoustic Society of America, 28 (2)*, 179-191, 1956 (b).
Bowles, F. A., Observations on attenuations and shear wave velocity in fine-grained, marine sediments *Journal of the Acoustic Society of America, 101 (6)*, 3385-3397, 1997
Brandes, H. G., Silva, A. J. and Sadd, M. H., Physical and acoustic measurements on cohesionlass sediments from the northwest Florida sand sheet. *Geophysical Research Letters, 28 (5)*, 823-826, 2001
Briggs, K. B. and Richardson, M. D., Small-scale fluctuations in acoustic and physical properties in surficial carbonate sediments and their relationship to bioturbation *Geo-Marine Letters, 17*, 306-315, 1997
Buckingham, M. J., Theory of compressional and shear waves in fluidlike marine sediments *Journal of the Acoustic Society of America, 103 (1)*, 288-299, 1998
Buckingham, M. J., Wave propagation, stress relaxation, and grain-to-grain shearing in saturated, unconsolidated marine sediments *Journal of the Acoustic Society of America, 108 (6)*, 2798-2815, 2000
Buckingham, M. J. and Richardson, M. D., On Tone-burst measurements of sound speed and atttenuation in sandy marine sediments *IEEE Journal of Oceanic Engineering, 27 (3)*, 429-453, 2002
Cascante, G., Propagation of mechanical waves in particulate materials, PhD, Civil Engineering, University of Waterloo, pp, 1996.
Courtney, R. C. and Mayer, L., Acoustic properties of fine-grained sediments from Emerald Basin: Toward an inversion for physical properties using Biot-Stoll model *Journal of the Acoustic Society of America, 93 (6)*, 3193-3200, 1993 (a).
Courtney, R. C. and Mayer, L. A., Calculation of acoustic parameters by a filter-correlation method. *Journal of the Acoustical Society of America, 93 (2)*, 1145-1154., 1993 (b).
Endo, H., Use of a power law relation to describe field measurements of compressional and shear velocity in a sediment *Journal of the Acoustic Society of America, 101 (4)*, 2378-2380, 1997
Evans, R. B. and Carey, W. M., Frequency dependence of sediment attenuation in two low-frequency shallow-water acoustic experimental datasets *IEEE Journal of Oceanic Engineering, 23 (4)*, 439-447, 1998
Ferry, J. D., Visco elastic properties of polymers, John Wiley, New York, 482 pp, 1961.
Frazer, L. N. and Fu, S. S., Seabed sediment attenuation profiles from a movable sub-bottom acoustic vertical array *Journal of the Acoustical Society of America, 106 (1)*, 120-130, 1999
Fry, J. C. and Riatt, R. W., Sound velocities at the surface of deep sea sediments *Journal of Geophysical Research, 66 (2)*, 589-597, 1961
Geertsma, J. and Smit, D. C., Some aspects of elastic wave propagation in fluid-saturated porous media *Geophysics, 26*, 169-181, 1961
Gei, D. and Carcione, J. M., Acoustical properties of sediments saturated with gas hydrate, free gas and water. *Geophysical Prospecting, 51 (2)*, 141-157, 2003
Gorgas, T. J., Wilkens, R. H., Fu, S. S., Frazer, L. N., Richardson, M. D., Briggs, K. B. and Lee, H., In situ acoustic and laboratory ultrasonic sound speed and attenuation measured in hetergoneous soft seabed sediments: Eel River shelf, California *Marine Geology, 182*, 103-119, 2002

Hamilton, E. L., Sound velocity and related properties of marine sediments, North Pacific. *Journal of Geophysical Research, 75 (23)*, 4423-4446, 1970
Hamilton, E. L., Bucker, H. P., Keir, D. L. and Whitney, J. A., Velocities of compressional and shear waves in marine sediments determined from a research vessel *Journal of the Acoustic Society of America, 75*, 4039-4049, 1970
Hamilton, E. L., Elastic Properties of Marine Sediments. *Journal of Geophysical Research, 76 (2)*, 579-603, 1971 (a).
Hamilton, E. L., Prediction of in-situ acoustic and elastic properties of marine sediments. *Geophysics, 36 (2)*, 266-284, 1971 (b).
Hamilton, E. L., Compressional-wave attenuation in marine sediments *Geophysics, 37 (4)*, 620-646, 1972
Hamilton, E. L., Sound velocity and related properties in marine sediments, North Pacific. *Journal of Geophysical Research, 75 (23)*, 4432-4446, 1975
Hamilton, E. L. and Bachman, R. T., Sound velocity and related properties in marine sediments *Journal of the Acoustic Society of America, 72 (6)*, 1891-1904, 1982
Hamilton, E. L., Acoustic properties of sediments, pp 4-58 in "Acoustics and the ocean bottom", eds: Carbo-Fite, C., 1987.
Hampton, L. D., Acoustical properties of sediments *Journal of the Acoustic Society of America, 42*, 882-890, 1967
Horn, D. R., Horn, B. M. and Delach, M. N., Correlation between acoustic and other physical properties of deep-sea cores *Journal of Geophysical Research, 73 (6)*, 1939-1957, 1968
Hovem, J. M. and Ingram, G. D., Viscous attenuation of sound in saturated sand *Journal of the Acoustic Society of America, 66 (6)*, 1807-1812, 1979
Hovem, J. M., Viscous attenuation of sound in suspensions and high-porosity marine sediments *Journal of the Acoustic Society of America, 67 (5)*, 1559-1563, 1980
Johnston, D. H., Toksoz, M. N. and Timur, A., Attenuation of seismic waves in dry and saturated rocks: II. Mechanics *Geophysics, 44 (4)*, 691-711, 1979
Johnston, D. L. and Plona, T. J., Acoustic slow waves and the consolidation transition *Journal of the Acoustic Society of America, 72 (556-565)*, 1982
Johnstone, D. H. and Toksoz, M. N., Definitions and terminology, pp 1-5 in "Seismic wave attenuation", eds: Johnstone, D. H., Society of Exploration Geophysics, 1981.
Kibblewhite, A. C., Attenuation of sound in marine sediments: A reveiw with emphasis on new low frequency data. *Journal of the Acoustical Society of America, 86 (2)*, 716-738, 1989
Kim, D. C., Sung, J. Y., Park, S. C., Lee, G. H., Choi, J. H., Kim, G. Y., Seo, Y. K. and Kim, J. C., Physical and acoustic properties of shelf sediments, the South Sea of Korea *Marine Geology, 179*, 39-50, 2001
LeBlanc, L. R., Panda, S. and Schock, S. G., Sonar attenuation modeling for classification of marine sediments *Journal of the Acoustical Society of America, 91 (1)*, 116-126, 1992 (a).
Leighton, T. G., The Acoustic Bubble, Academic Press Limited, London, 613 pp, 1994.
Leurer, K. C., Attenuation in fine-grained marine sediments: Extension of the Biot-Stoll model by the "effective grain model" (EGM) *Geophysics, 62 (5)*, 1465-1479, 1997
Lewis, L. F., An investigation of ocean sediments using the deep ocean sediment probe, PhD, Department of Ocean Engineering, University of Rhode Island, pp, 1971.

Lu, T., Bryant, W. R. and Slowey, N. C., Regression analysis of physical and geotechnical properties of surface marine sediments *Marine Georesources and Geotechnology, 16*, 201-220, 1998 (a).
Marion, D., Nur, A., Yin, H. and Han, D., Compressional velocity and porosity in sand-clay mixtures *Geophysics, 57 (4)*, 554-563, 1992
McCann, C., An investigation of the acoustic properties of natural materials, PhD, Department of Physical Oceanography, University College of North Wales, 308 pp, 1967.
McCann, C. and McCann, D. M., A theory of compressional wave attenuation in noncohesive sediments *Geophysics, 50 (8)*, 1311-1317, 1985
McCann, D. M. and McCann, C., The attenuation of compressional waves in marine sediments *Geophysics, 34 (6)*, 882-892, 1969
McLeroy, E. G. and DeLoach, A., Sound speed and attenuation, from 15 to 1500 kHz, measured in natural seafloor sediments *Journal of the Acoustical Society of America, Letters to the editor*, 1148-1150, 1968
McManus, J., Grain size determination and interpretation, pp 63-85 in "Techniques in Sedimentology", eds: Tucker, M., Blackwell Scientific Publications, 1989.
Molis, J. C. and Chotiros, N. P., A measurement of the grain-bulk-modulus of sand *Journal of the Acoustic Society of America, 91 (4)*, 2463, 1992
Murphy, W. F., Acoustic Measures of Partial Gas Saturation in Tight Sandstones *Journal of Geophysical Research, 89 (B13)*, 11549-11559, 1984
Nafe, J. E. and Drake, C. L., Physical properties of marine sediments, pp 794-815 in "The Sea", eds: Hill, M. N., Interscience, 1963.
Neprochnov, Y. P., Seismic studies of the crustal structure beneath the seas and oceans *Oceanology (English translation), 11*, 709-715, 1971
Nur, A., Marion, D. and Yin, H., Wave velocities in sediments, pp 131-140 in "Shear waves in marine sediments", eds: Hovem, J. M., Kluwer Academic Publishers, 1991.
Orsi, T. H. and Dunn, D. A., Sound velocity and related physical properties of fine-grained abyssal sediments from the Brazil Basin (South Atlantic Ocean) *Journal of the Acoustic Society of America, 88 (3)*, 1536-1542, 1990
Orsi, T. H. and Dunn, D. A., Correlations between sound velocity and related properties of Glacio-Marine sediments: Barents Sea *Geo-Marine Letters, 1*, 79-83, 1991
Plona, T. J., Observation of a second bulk compressional wave in a porous medium at ultrasonic frequencies *Applied Physics letters, 36*, 259-261, 1980
Richardson, M. D. and Briggs, K. B., On the use of acoustic impedance values to determine sediment properties *Proceedings to the Institute of Acoustics, 15 (2)*, 15-23, 1993
Richardson, M. D., Lavoie, D. L. and Briggs, K. B., Geoacoustic and physical properties of carbonate sediments of the Lower Florida Keys *Geo-Marine Letters, 17*, 316-324, 1997
Richardson, M. D., Williams, K. L., Briggs, K. B. and Thoros, E. I., Dynamic measurement of sediment grain compressibility at atmospheric pressure : acoustic applications *IEEE Journal of Oceanic Engineering, 27 (3)*, 593-601, 2002
Rodgers, A. K., Yamamoto, T. and Carey, W., Experimental investigation of sediment effect on acoustic wave propagation in the shallow ocean *Journal of the Acoustic Society of America, 93 (1747-1761)*, 1993
Shumway, G., Sound speeds and absorption studies of marine sediment by a resonance method *Geophysics, 25 (2)*, 451-467, 1960
Shumway, G. and Igelman, K., Computed sediment grain surface areas *Journal of Sedimantary Petrology, 30 (486-489)*, 1960

Simpson, H. J., Houston, B. H., Liskey, S. W., Frank, P. A., Berdoz, A. R., Kraus, L. A., Frederickson, C. K. and Stanic, S., At-sea measurements of sound penertraion into sediments using a buried vertical synthetic array *Journal of the Acoustic Society of America, 114 (3)*, 1281-1290, 2003
Stevenson, I. R., McCann, C. and Runciman, P. B., An attenuation-based sediment classification technique using Chirp sub-bottom profiler data and laboratory acoustic analysis *Marine Geophysical Researches, 23*, 277-298, 2002
Stoll, R. D. and Bryan, G. M., Wave attenuation in saturated sediments *Journal of the Acoustic Society of America, 47 (5)*, 1440-1447, 1970
Stoll, R. D., Sediment Acoustics, Lecture Notes in Earth Science 26, Springer-Verlag, 153 pp, 1974.
Stoll, R. D., Acoustic waves in saturated sediments, pp 19-39 in "Physics of sound in marine sediments", eds: Hampton, E. L., Plenum Press, 1974.
Stoll, R. D., Sediment Acoustics, Leture Notes in Earth Science Springer-Verlag, 153 pp, 1974.
Stoll, R. D., Acoustic waves in ocean sediments *Geophysics, 42 (4)*, 715-725, 1977
Stoll, R. D., Experimental studies of attenuation in sediments *Journal of the Acoustic Society of America, 66 (4)*, 1152-1161, 1979
Stoll, R. D., Marine sediment acoustics *Journal of the Acoustic Society of America, 77 (5)*, 1789-1799, 1985
Stoll, R. D. and Bautista, E. O., Using the Biot model to establish a baseline geoacoustic model for seafloor sediments *Continental Shelf Research, 18*, 1839-1857, 1998
Stoll, R. D., Velocity dispersion in water-saturated granular sediment *Journal of the Acoustic Society of America, 111 (2)*, 785-793, 2001
Sutton, G. H., Berckhemer, H. and Nafe, J. E., Physical analysis of deep sea sediments. *Geophysics, 22 (4)*, 779-812, 1957
Tittmann, B. R., Internal friction measurements and their implications in seismic Q structure models of the crust, pp 81-97 in "Seismeic wave attenuation", eds: Toksoz, M. N. and Johnson, D. H., Society of exploration Geophysicists, 1981.
Tuffin, M., The geoacoustic properties of shallow gas bearing sediments, PhD, School of Ocean and Earth Science, University of Southampton, 149 pp, 2001.
Turgut, A. and Yamamoto, T., Measurements of acoustic wave velocities and attenuation in marine sediments *Journal of the Acoustic Society of America, 87 (6)*, 2376-2383, 1990
Williams, J. and Elder, S. A., Fluid phyiscs for oceanographers and physicists, Pergamon, 300 pp, 1989.
Williams, K. L., Jackson, D. P., Thoros, E. I., Tang, D. and Schock, S., Comparison of sound speed and attenuation measured in a sandy sediment to predictions based on the Biot theory of porous material *IEEE Journal of Oceanic Engineering, 27 (3)*, 413-428, 2002
Wingham, D. J., The dispersion of sound in sediment *Journal of the Acoustical Society of America, 78 (5)*, 1757-1760, 1985
Winkler, K. and Nur, A., Pore fluids and seiesmic attenuation in rocks. *Geophysical Research Letters, 6*, 1-4, 1978
Winkler, K. W. and Plona, T. J., Techniques for measureing ultrasonic velocity and attenuation spectra in rocks under pressure *Journal of Geophysical Research, 87 (10776-10780)*, 1982
Wood, A. B., A textbook of sound, G. Bell and Sons, London, pp, 1941.

Wood, A. B. and Weston, D. E., The propagation of sound in mud *Acustica, 14*, 156-162, 1964
Wylie, M. R. J. and Gregory, A. R., Fluid flow through unconsolidated porous agregates, effect of porosity and particle shape on Kozeny-Carman constants *Industial Engineering Chemistry, 47 (1379-1388)*, 1955